



Cite this: DOI: 10.1039/d0cs01019g

## Towards development of a novel universal medical diagnostic method: Raman spectroscopy and machine learning†

Nicole M. Ralbovsky <sup>ab</sup> and Igor K. Lednev \*<sup>ab</sup>

Many problems exist within the myriad of currently employed screening and diagnostic methods. Further, an incredibly wide variety of procedures are used to identify an even greater number of diseases which exist in the world. There is a definite unmet clinical need to improve diagnostic capabilities of these procedures, including improving test sensitivity and specificity, objectivity and definitiveness, and reducing cost and invasiveness of the test, with an interest in replacing multiple diagnostic methods with one powerful tool. There has been a recent surge in the literature which focuses on utilizing Raman spectroscopy in combination with machine learning analyses to improve diagnostic measures for identifying an assortment of diseases, including cancers, viral and bacterial infections, neurodegenerative and autoimmune disorders, and more. This review highlights the work accomplished since 2018 which focuses on using Raman spectroscopy and machine learning to address the need for better screening and medical diagnostics in all areas of disease. A critical evaluation considers both the benefits and obstacles of utilizing the method for universal diagnostics. It is clear based on the evidence provided herein Raman spectroscopy in combination with machine learning provides the first glimmer of hope for the development of an accurate, inexpensive, fast, and non-invasive method for universal medical diagnostics.

Received 7th August 2020

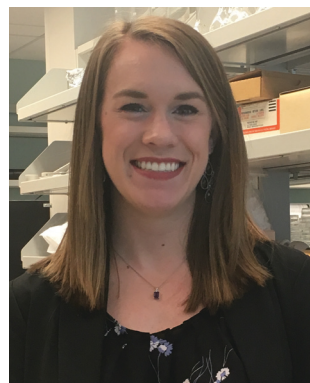
DOI: 10.1039/d0cs01019g

rsc.li/chem-soc-rev

<sup>a</sup> Department of Chemistry, University at Albany, SUNY, 1400 Washington Avenue, Albany, NY 12222, USA. E-mail: [ilednev@albany.edu](mailto:ilednev@albany.edu); Tel: +1 518 591 8863

<sup>b</sup> The RNA Institute, University at Albany, SUNY, 1400 Washington Avenue, Albany, NY 12222, USA

† Electronic supplementary information (ESI) available. See DOI: 10.1039/d0cs01019g



**Nicole M. Ralbovsky**

Nicole M. Ralbovsky received her BSc in 2016 from the State University of New York at Geneseo and will receive her PhD in December 2020 from the University at Albany, State University of New York, under the supervision of Prof. Igor K. Lednev. Nicole will join the lab of Dr Joseph Smith as a post-doctoral scientist at Merck & Co. Her research has focused on utilizing Raman spectroscopy in combination with machine

learning for medical diagnostic applications. Nicole has been the recipient of several prestigious student awards including the Coblenz Society Award, Eastern Analytical Symposium Research Award, and NY/NJ Society for Applied Spectroscopy Award.



**Igor K. Lednev**

Igor K. Lednev is a Professor at the University at Albany, State University of New York. He received his PhD from the Moscow Institute of Physics and Technology. His research is focused on the development and application of novel laser spectroscopy for medical diagnostics and forensic purposes. Dr Lednev is a cofounder of two startup companies commercializing his patented technology. He served

as an advisory member on the White House Subcommittee for Forensic Science. He is a Fellow of the Royal Society of Chemistry and Society for Applied Spectroscopy. He co-authored about 240 publications in peer-reviewed journals and 7 patents.

## 1. Introduction

Receiving a diagnosis for an ailment is an event nearly every individual in the world will experience at least once in their lifetime. Whether the illness is a viral infection, blood disorder, or cancer, early and accurate detection is at the heart of properly treating and aiding the afflicted individual. However, just as the diseases a person can contract are diverse, so too are the methods utilized for screening and diagnosing them. Within these various techniques lies significant room for improving measures such as the test's sensitivity and specificity, its access and availability, and its definitiveness, as well as reducing the cost, time to perform, and level of invasiveness associated with the test. To address these needs, there has been a strong push toward developing a novel method which can be applied for universal medical diagnostics; that is, the development of a minimally invasive single test which can simply and accurately screen for as well as diagnose a wide variety of illnesses and diseases early-on while also being time-efficient and cost-effective. Raman spectroscopy (RS) is proposed here as a method which can satisfy this massively important role.

Raman spectroscopy is an exceptional analytical tool used for obtaining very specific information regarding a sample's molecular composition. RS involves the irradiation of a sample by a monochromatic light source. Incident photons of light will interact with the sample, causing excitation and deactivation of molecular vibrations as a result of inelastic, or Raman, scattering. The energy difference between the incident and scattered photons is thus equivalent to the energy of numerous molecular vibrations in the sample. Thus, RS is said to provide a vibrational "fingerprint" of the sample that is known to be the most specific spectroscopic characteristic of the material.

RS provides incredible detail regarding the biochemical composition of a biological sample; due to its specificity, it is expected that RS will be able to determine differences between biological samples collected from healthy and diseased donors. Further, it can collect and process spectral information from multiple positions on a sample with the purpose of providing statistically significant characterization of the sample's heterogeneity and multicomponent composition. This creates the opportunity to detect multiple biomarkers simultaneously, which most diagnostic tests and exams are not capable of doing. In addition to its specificity, RS has considerable advantages over other methods used for diagnostics. The method is inherently non-invasive and can be used *in vivo* due to the advent of handheld instruments and fiber-optic probes. RS is not expensive in comparison to diagnostic imaging tests, and it is objective, which makes it a more desirable tool over diagnostic methods which require human interpretation of the results, such as histopathology. Most importantly, RS is easy-to-use, fast, reliable, and can simply be adapted for use in clinical settings.

It is important to note the changes which occur between spectra of different biological samples can oftentimes be small and not easily observable. As a result, chemometrics, or machine learning, is frequently used to interpret the collected spectral data. The application of chemometrics to data which

exists as a matrix, such as Raman spectral data, allows the user to generate machine learning prediction algorithms for the purpose of sorting and separating chemical data. Specifically, the prediction algorithms learn similarities and differences between classes of data, such as that obtained from biological samples of healthy donors and donors with a disease. Once the model is built using known data, it can then be applied toward making a classification prediction on new, unknown, data presented to it. In this way, these algorithms can be used for specific and accurate medical screening and diagnostic purposes.

There are many different chemometric methods which exist to answer a variety of scientific questions. Specifically, there are two main types of statistical models that can be built: supervised and unsupervised models. Techniques which are unsupervised do not utilize user-defined information during model construction; these types of methods tend to be exploratory in nature and are sufficient for separating dissimilar sets of data while grouping together data that is similar. Examples of unsupervised methods include principal component analysis and *K*-means cluster analysis. The other category of models is called supervised methods because these do consider user-defined information, such as class labels. Within supervised methods, regression models and classification models exist. Regression models, such as logistic regression, can compare Raman spectral data to changes in time or concentration, for example, and thus function similarly to the ideas of calibration curves. Classification techniques are known to yield qualitative responses, such as the class of a donor. Examples of supervised classification methods include partial least squares and support vector machine discriminant analyses. Chemometric methods have been applied to solve a variety of issues using Raman spectroscopy and its variations.<sup>1–3</sup> Table 1 provides a brief overview of commonly used methods discussed herein; for a more detailed review of chemometric methods, including various advantages and disadvantages of the methods, the reader is referred to other works which go into greater detail.<sup>4–7</sup>

Validation of the chemometric model is required after it has been built. Receiver operating characteristic curves are sometimes used for illustrating the ability of a binary classification system to make a correct classification as its discrimination threshold is varied. Further, there are two main variations of validation. Cross validation implies a validation scheme where the spectral data that is used to build the model is also used to test its prediction abilities. This can be done in several ways; the most common include leave-one-spectrum-out, leave-one-sample-out, and *k*-fold cross validation. The first and second methods involve leaving either a single spectrum or all spectra from one sample out of the model building process. The left-out data is used to test the performance of the model. This process is then repeated until all data has been left out. Similarly, *k*-fold cross-validation randomly divides the data set into *k* groups and builds the model with *k* – 1 groups. The leftover group is again repeatedly used for evaluating its performance. The second type of validation is called independent or external validation. This method evaluates the performance of the model on data that was not used to build it. This type of validation indicates whether or

**Table 1** Brief introduction to commonly used chemometric methods

Method	Function	Description
ANN	Classification and regression analysis	Computing system consisting of a collection of connected units called artificial neurons; input neurons connect to a defined number of hidden layers, which subsequently connect to an output layer which generates the class prediction
GA	Optimization methodology	Generates evolved solutions by relying on biological operators including selection, mutation, and cross-over
KNN	Classification and regression analysis	Determines an unknown case by comparing the distance of the unknown to all stored available cases
LDA	Dimensionality reduction and classification analysis	Recognizes the ideal linear combination of features which characterizes or separates two or more classes of objects
PCA	Unsupervised feature extraction and dimensionality reduction	An orthogonal transformation of the original dataset into a reduced subspace of features with eigenvalues describing their importance in decreasing order of explained variance
PLS-DA	Dimensionality reduction and classification analysis	Linear classification model which projects predicted variables and observable variables into a new space
RF	Classification and regression analysis	Constructs many decision trees during training; the output classification of a new sample is the mean prediction of all trees
SVM	Classification and regression analysis	Determines the hyperplane which maximizes the distance between classes while minimizing misclassifications

not a model was over-fit and allows the builder to determine how it may perform in further clinical applications. The results of external validation are crucial to pushing the method toward real-world use.

Due to their significant advantages independently as well as combined, abundant research has been published on screening and diagnosing a wide range of diseases using Raman spectroscopy and chemometric techniques. In addition to research articles, reviews have been conducted which address the topic of RS for medical diagnostics. However, an updated review is necessary. Upon investigating reviews published in 2014 or later, many informative documents were written which emphasized different aspects of the topic at hand. For example, some review articles evaluated analytical techniques beyond RS;<sup>8–11</sup> on the other hand, several others review manuscripts specifically published using surface enhanced Raman spectroscopy<sup>12–16</sup> or fiber-optic probes, alone.<sup>17</sup> In some, specialized clinical areas are investigated including oncology<sup>18–22</sup> and regenerative medicine.<sup>23</sup> While some reviews differ in their level of conclusiveness,<sup>24,25</sup> others are comprehensive but are outdated and require an update on the current literature.<sup>26–29</sup> The reader is suggested to investigate these alternative and excellent reviews for further information on the aforementioned specialized topics.

The intention of this review is to fill in the necessary gap in the literature and provide a fully comprehensive review of manuscripts published during and after 2018. A review of this nature is critical and necessary to keep the field moving forward. Because of the immense potential of the method for solving a number of screening and diagnostic issues, it is incredibly important and useful to inform the community of the progress which has already been made to establish the steps leading to future productive work, including fully introducing the methodology into clinical settings. Specifically, articles which utilize RS and chemometric techniques for the purpose of screening or diagnosing any and all illnesses or diseases will be reviewed. Both SERS and spontaneous RS will be considered, as well as any research conducted using fiber-optic probes. Other variations of RS will also be considered if used in

conjunction with chemometric techniques. In this regard, only research which incorporates chemometric and machine learning methods will be considered. In order to bring the methodology into clinical settings, it is anticipated that an automatic data analysis procedure will be required to examine Raman spectral data and generate a diagnosis. Chemometrics can be performed using easily available software and can provide a rapid, definitive, and accurate diagnosis quickly and cost-effectively, thereby improving significantly upon the current methods used for diagnostics. The goal of this review is to promote and declare RS in combination with chemometrics as being a highly suitable universal method for medical diagnostics and screening applications. A critical evaluation of the benefits and risks of the method as well as comparisons between various studies will be included within the review in an effort to create a platform from which future work can successfully be accomplished.

## 2. Spontaneous Raman spectroscopy

Spontaneous Raman spectroscopy employs a laser which emits monochromatic light typically in the visible to near-infrared range. Photons from the laser light interact with the molecules within the irradiated sample and the resultant inelastically scattered photons are detected by the instrument in a quantitative way. The Raman spectrum that is produced is very specific to the sample in a manner similar to the uniqueness and specificity of a human fingerprint. Spontaneous RS permits detection and characterization of the multicomponent composition of a heterogeneous sample, making it useful for studying various biological samples. Typically, multiple spectra are collected from a single sample to better account for this heterogeneity. One of the most notable advantages of RS is its ability to integrate multiple potential biomarkers into one spectroscopic signature, thus improving the sensitivity and specificity of the method. Many different studies have utilized spontaneous RS for assessing its ability to diagnose a variety of diseases including cancers, infectious diseases, blood disorders, neurodegenerative diseases, and

more. Those studies which have done so in 2018 and beyond are reviewed here.

## 2.1. Cancer

The greatest number of studies have focused on accomplishing the detection of various forms of cancer within various biological samples. In one study, the tumor suppressor wild type p53 protein, considered a cancer biomarker, was investigated by Hernández-Vidales *et al.* Principal component analysis (PCA) and support vector machine (SVM) algorithms showed that the wild type and the mutant type of this biomarker were separated with 94% accuracy after leave-one-out cross-validation (LOOCV); the limit of detection of the wild type p53 was found to be 0.946  $\mu\text{M}$ , opening the door for applying this method for investigating any cancer using spontaneous RS.<sup>30</sup>

**Bladder cancer.** In a study led by Bovenkamp *et al.*, optical coherence tomography (OCT) was used in combination with RS for identifying different stages and grades of bladder cancer through the analysis of bladder tissue samples from eight donors. Degenerated tissue was first identified by OCT; RS was then used to determine molecular characteristics at suspicious sites. K-Nearest neighbor (KNN) with five-fold cross-validation (CV) was used to analyze OCT data, achieving 71% accuracy for staging a tumor; analysis of RS data achieved 93% accuracy for discriminating between low- and high-grade lesions *via* PCA followed by KNN, indicating RS as a preferred method for identifying the cancer.<sup>31</sup>

**Brain cancer.** Brain cancer was investigated by several different research groups. Tissue from grade IV medulloblastoma was compared to non-tumor samples from five individuals; results of partial least squares discriminant analysis (PLS-DA) with CV gave a sensitivity and specificity of 96.3% and 92%, respectively. Atomic force microscopy (AFM) was used to further recognize the heterogeneous mechanical properties of the tissue.<sup>32</sup> Mehta *et al.* investigated meningioma, a primary brain and central nervous system tumor. RS was used to classify blood serum from 35 control and 35 meningioma subjects; PCA combined with PC-linear discriminant analysis (PC-LDA) yielded 92% and 80% classification efficiencies for healthy and meningioma subjects, respectively, after leave-one-sample-out cross-validation (LOSOCV).<sup>33</sup> In a three-tiered study, brain metastases from primary adenocarcinomas of the lung ( $n = 7$ ) and colorectum ( $n = 7$ ) were analyzed in comparison to metastatic melanoma ( $n = 7$ ). PCA in combination with a linear discriminant classifier gave rise to classification accuracies of 69% for colorectal adenocarcinoma, 69% for lung carcinoma, and 72% for melanoma. A comparison to ATR-FTIR spectroscopy was made, where the same statistical analysis method resulted in accuracies of 60% for colorectal adenocarcinoma, 59% for lung carcinoma, and 47% for melanoma. Interestingly, when the two adenocarcinoma groups were combined, the classification accuracies increased to 85% for adenocarcinoma and 75.4% for melanoma using the Raman spectral data. It should be noted, however, that no validation was reported.<sup>34</sup> Depciuch *et al.* also compared the usefulness of FTIR spectroscopy *versus* RS for investigating chemical changes in brain tissues and glioblastoma tumor tissues. Data collected from cancer and marginal brain tissues

using both methods showed significant differences in chemical composition when compared to control brain tissues. PCA indicated these observed changes were significant for differentiating infected and healthy tissue as well as between adjacent brain tissue and control tissue. This research opens the door for further analysis of the data for diagnostic applications as well as for a better understanding of the biochemical changes which occur during cancer progression.<sup>35</sup> Zhou *et al.* utilized RS for differentiating brain metastases of lung cancer adenocarcinoma (ADC) and squamous cell carcinoma (SCC) from normal tissue (Fig. 1). The results of optical spatial frequency spectroscopy analysis, which determines the difference in random spatial frequency structures in micrograph images of the tissues, combined with RS was examined using SVM and receiver operating characteristic (ROC) curve analysis. All three types of brain tissue were identified with high levels of accuracy; further, normal and cancerous tissues were discriminated in a binary model with 88.5% sensitivity and 75% specificity with an area under the ROC curve (AUC) of 0.93; validation is needed to further support the results.<sup>36</sup> The best outcomes were obtained when tissue was analyzed using a simple PC-LDA classifier.

**Breast cancer.** Attempts to investigate breast cancer were frequent. An ant colony optimization (ACO) algorithm was used to improve the power of breast cancer diagnosis by RS. Spectra from normal ( $n = 3$ ), benign ( $n = 5$ ), and cancerous ( $n = 3$ ) breast tissue was collected. ACO identified five features which were optimum for diagnosis, and quadratic discriminant analysis (QDA) resulted in 87.7% accuracy for differentiating between the three types of tissue after LOOCV.<sup>37</sup> Marro *et al.* compared the ability of multivariate curve resolution (MCR) *versus* PCA for deconvolution of the meaningful components of the spectral dataset of breast cancer cells. The MCR algorithm combined with alternating least squares (ALS) analysis showed a strong ability to monitor the progression of breast cancer cells to bone metastasis, providing crucial biochemical insights into the molecular progression of cancer cells as compared to PCA. Further, two cell lines (BO2 and MDA-MB-435P) were discriminated from each other using PLS-DA with CV, reaching 100% specificity and 90% specificity, respectively.<sup>38</sup> In another study, the ability of RS to discriminate between benign lesions and cancer tissue of 20 different donors was investigated. Several different chemometric methods were applied to the spectral dataset; PCA-LDA, PCA-QDA, and PLS-DA all achieved > 80% sensitivity and specificity for classification whereas PCA-SVM achieved > 90% sensitivity and specificity after external validation.<sup>39</sup> In a unique study, white light interference microscopy (WLIM) was combined with RS in an attempt to differentiate between 80 cancerous and normal breast tissue samples collected from 16 patients. WLIM provided quantitative phase information about the samples whereas RS detected the molecular changes occurring during cancer progression. A SVM classifier was built to classify the tissue samples; a ROC curve was used to check the accuracy of the model, which achieved 90.6% accuracy for cancer detection during external validation.<sup>40</sup> Talari *et al.* studied breast cancer tissue using RS in conjunction with PCA and LDA. LDA classified biopsies into luminal A, luminal B, HER2, and triple negative subtypes with

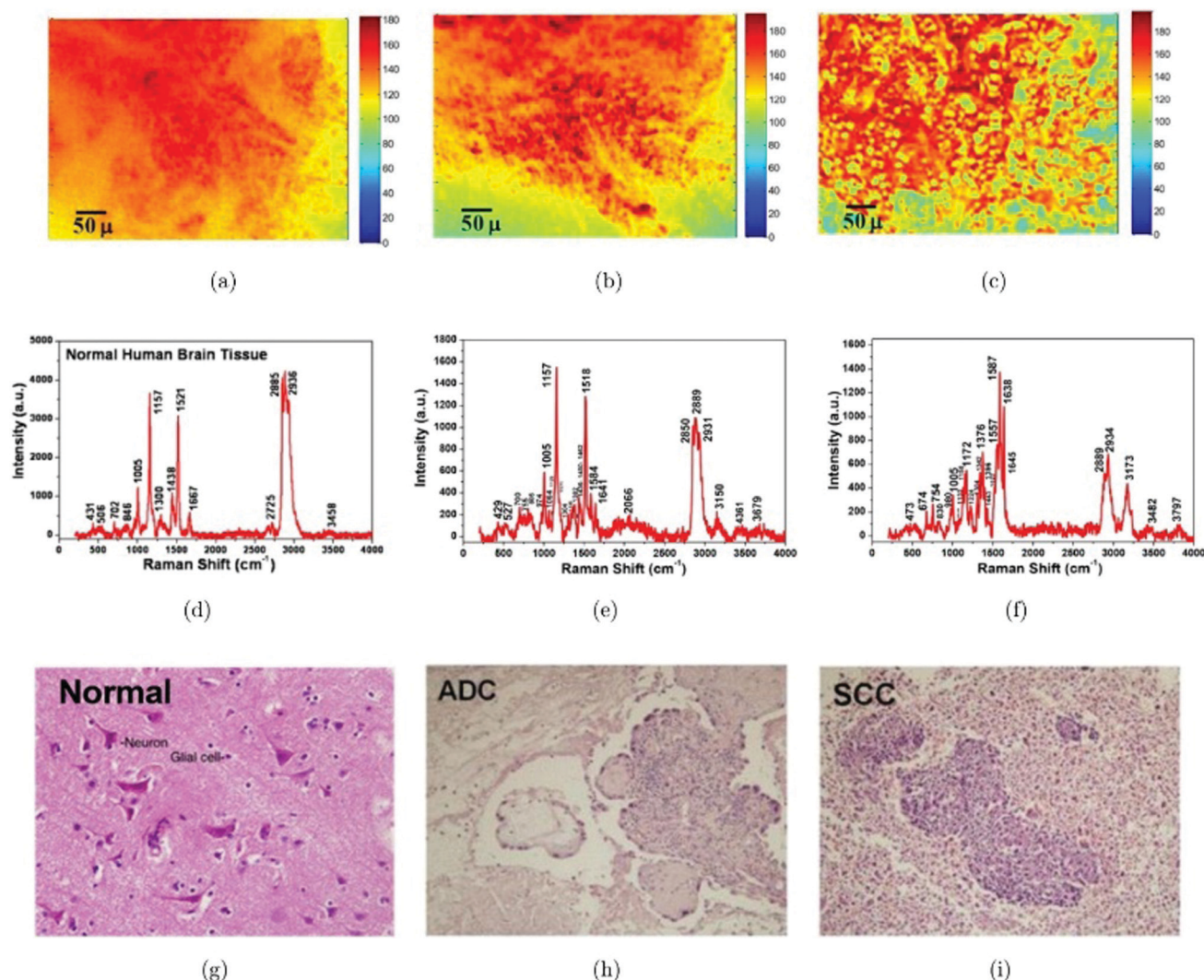


**Fig. 1** Three sets of data from brain metastases of lung cancer and normal tissue. Upper row: A set of typical cropped confocal micrograph images using pseudo color of (a) normal brain tissue, (b) brain metastasis from ADC, and (c) brain metastasis from SCC. Middle row: A set of Resonance Raman spectra of (d) normal brain tissue, (e) brain metastasis from ADC and (f) brain metastasis from SCC. The spectra in (d)–(f) are corresponding to the images in (a)–(c), respectively. Bottom row: H&E-stained images from (g) normal brain tissue, (h) brain metastasis from ADC and (i) brain metastasis from SCC. All the H&E images used 20 $\times$  objective and correspond to the images in (a)–(c), respectively. Reprinted with permission from Y. Zhou, C.-H. Liu, Y. Pu, B. Wu, T. A. Nguyen, G. Cheng, L. Zhou, K. Zhu, J. Chen, Q. Li, R. R. Alfano, Combined spatial frequency spectroscopy analysis with visible resonance Raman for optical biopsy of human brain metastases of lung cancers, *J. Innov. Opt. Health Sci.*, 2019, **12**(2), 1950010. Copyright (2019) World Scientific Publishing Company.

an average accuracy of 89.2% after CV.<sup>41</sup> Alternatively, RS and an orthogonal partial least squares (OPLS) discriminant analysis algorithm could successfully separate data obtained from healthy and invasive ductal carcinoma in breast tissue samples based on cluster analysis with a very low root mean square error of CV (0.09).<sup>42</sup> Of the studies which examined tissue, varying results were achieved, indicating the importance of selecting the optimum chemometric technique for analyzing spontaneous RS data.

The analysis of body fluids was used in additional reports for diagnosing breast cancer. PCA-LDA could discriminate between blood plasma of normal ( $n = 26$ ) and breast cancer ( $n = 19$ ) subjects, achieving 100% classification accuracy after LOSOCV. Further, ROC curve analysis of spectral variations of various

biomolecules, including phenylalanine, proteins, and lipids, resulted in 100% sensitivity and 83–100% specificity for classification.<sup>43</sup> Blood plasma of breast cancer patients and healthy controls was also investigated by another group; PCA-factorial discriminant analysis (FDA) with CV could classify all blood plasma samples from breast cancer donors ( $n = 18$ ) with 100% specificity and 99% sensitivity when compared to healthy controls ( $n = 8$ ). Further, PCA-FDA successfully differentiated stage II and stage III breast cancer with 94% specificity and 95% sensitivity, and stage II and stage IV breast cancer with 100% specificity and 90% sensitivity, indicating the potential of the method for achieving early diagnosis and staging of breast cancer.<sup>44</sup> Interestingly, blood plasma seemed to provide more biochemical information than the tissue samples, resulting in better prediction accuracies.

**Cervical cancer.** Several studies were published on efforts to identify cervical cancer. PCA and artificial neural networks (ANN) with CV were used in one study to discriminate between normal ( $n = 64$ ), neoplastic ( $n = 36$ ), and malignant ( $n = 145$ ) cells/tissues with 99% accuracy. PC-LDA with CV was then used to separate well differentiated, moderately differentiated, and poorly differentiated SCC with 94.0% accuracy, demonstrating the potential of RS to replace histopathology.<sup>45</sup> Cells were again analyzed in a different study; high grade squamous intraepithelial (HSIL) cells were investigated through analysis of HSIL-associated biochemical changes in normal appearing intermediate and superficial cells using RS. PLS-DA with CV could diagnose HSIL compared to intermediate, superficial, and mixed intermediate/superficial cells with an average sensitivity of 95.6% and specificity of 93.6%, suggesting morphologically normal appearing cells can be used to identify the differences between negative and HSIL cytology.<sup>46</sup> In a different report, 95 total cervical adenocarcinoma and cervical SCC tissues were distinguished from each other with 93.1% accuracy using PCA-SVM with external validation.<sup>47</sup> On the other hand, blood plasma of 30 normal and 18 cervical cancer patients was separated using PCA-LDA with 94.4% sensitivity and 96.7% specificity after LOOCV; ROC curve analysis yielded 100% accuracy.<sup>48</sup> The aforementioned reports indicate that regardless of the biological sample studied, respectable diagnostic performance can be achieved through analysis of spontaneous RS data for detecting cervical cancer.

**Colorectal cancer.** Spontaneous RS was investigated for its potential to diagnose colorectal cancer through analysis of two different colorectal cancer cell lines (SW480 and SW620). PCA with LDA yielded an accuracy of 98.7% for classification. Further, five different cell lines (HL60, HT29, HCT116, SW620, and SW480) were separated using PCA-LDA with 92.4% accuracy, suggesting cells as a preferred biological sample for identifying colorectal cancer. Both analyses were verified using 10-fold CV.<sup>49</sup>

**Esophageal cancer.** Maitra *et al.* examined whether RS could interrogate various body fluids for the purpose of detecting different stages of esophageal adenocarcinoma, including normal/squamous epithelium, inflammatory, Barrett's, low-grade dysplasia (LGD), high-grade dysplasia (HGD), and esophageal adenocarcinoma (OAC). A combination of genetic algorithm (GA) with QDA resulted in 100% separation of all classes using saliva and urine samples after external validation. Plasma and serum samples could be classified with >90% accuracy for all esophageal stages. This study poses an interesting comparison of different body fluids and their potential for diagnosing the same disease.<sup>50</sup>

**Gastric cancer.** Bahreini *et al.* investigated RS for distinguishing between blood serum samples of 40 healthy controls and 20 patients with gastric cancer using PLS-DA. Results of CV yielded 87.5% classification efficiency, presenting RS analysis of serum as a potential screening tool for gastric cancer.<sup>51</sup> These results were comparable to those reported further on using SERS.

**Head and neck cancers.** Khan *et al.* studied nasopharyngeal cancer (NPC) via analysis of blood serum from 15 healthy controls and 14 NPC patients. SVM classification resulted in 93% accuracy after CV.<sup>52</sup> Larynx cancer was evaluated through

analysis of healthy ( $n = 13$ ) and cancerous ( $n = 13$ ) tissues. Raman spectral data was subjected to OPLS with CV, and the generated algorithm successfully clustered healthy and cancerous tissue spectra.<sup>53</sup> Furthermore, inverted papillomas, tumors of the sinonasal tract, were analyzed by RS. Three different types of sinonasal tissues were explored using PCA-LDA; the model effectively distinguished between normal sinonasal mucosa, chronic rhinosinusitis, and inverted papilloma tissue with an average accuracy of 90.2%; a validation scheme was not reported.<sup>54</sup>

**Leukemia.** The diagnosis of leukemia was examined by Managò *et al.* Initially, different leukocyte subpopulations of lymphocytes (B, T, and NK cells) as well as monocytes and granulocytes were identified using PCA and LDA with about 99% accuracy after LOOCV. Secondly, normal B cells and transformed MN60 lymphocyte leukemic cell lines were efficiently separated *via* the same procedure.<sup>55</sup> In a different study, an attempt was made to differentiate between 7 leukemia, 16 breast cancer, and 22 cervical cancer blood serum donors by super paramagnetic clustering and PCA, which was found to be successful.<sup>56</sup> Lastly, the differences of whole blood ( $n = 38$ ) and plasma ( $n = 40$ ) samples taken from healthy controls and leukemic subjects were investigated using RS. PLS was used to build discriminatory models, yielding 91.9% sensitivity and 100% specificity for classifying whole blood spectra. The plasma spectra were separated with 95.7% sensitivity and 98% specificity after LOSOCV, demonstrating the ability of RS to diagnosis acute leukemia in both whole blood and plasma samples with similar levels of success (Fig. 2).<sup>57</sup>

**Lung cancer.** Lung cancer was investigated using spontaneous RS in three recent manuscripts. Wang *et al.* measured Raman spectra from blood serum of healthy volunteers ( $n = 14$ ) and patients with different stages of non-small cell lung cancer (NSCLC,  $n = 77$ ). PCA-LDA with CV separated healthy, stage I, stage II, and stage III/IV NSCLC serum samples with an average of 78.3% sensitivity and 92.5% specificity; the overall accuracy was 92%.<sup>58</sup> Alternative research focused on using two different excitation wavelengths for identifying lung cancer in normal, non-cancerous abnormal, and cancerous tissue from 32 patients. LDA with CV showed 84% accuracy for discrimination using FT-Raman ( $\lambda_{\text{ex}} = 1064$  nm) and 100% accuracy with the standard 785 nm excitation after CV, indicating a strong preference for near-IR excitation.<sup>59</sup> Zheng *et al.* used SVM and KNN to cytopathologically diagnose lung cancer with almost 99% accuracy; no validation was reported.<sup>60</sup> Generally, the different biological samples employed in these reports provided similar levels of biochemical information which could be used for differentiation.

**Lymphatic cancers.** B-cell non-Hodgkin lymphoma was studied through RS for the purpose of distinguishing normal B-cells and B-cell non-Hodgkin lymphoma cells. PCA showed successful clustering of the two different cell types as well as between different types of B-cell non-Hodgkin lymphoma cells, indicating the potential of the method for analyzing tumor cells.<sup>61</sup> Related, lymph nodes of 20 patients affected by different conditions including reactive follicular hyperplasia (benign), follicular lymphoma (low grade primary tumor), diffuse B cell lymphoma (high grade primary tumor), and tumor metastasis (secondary

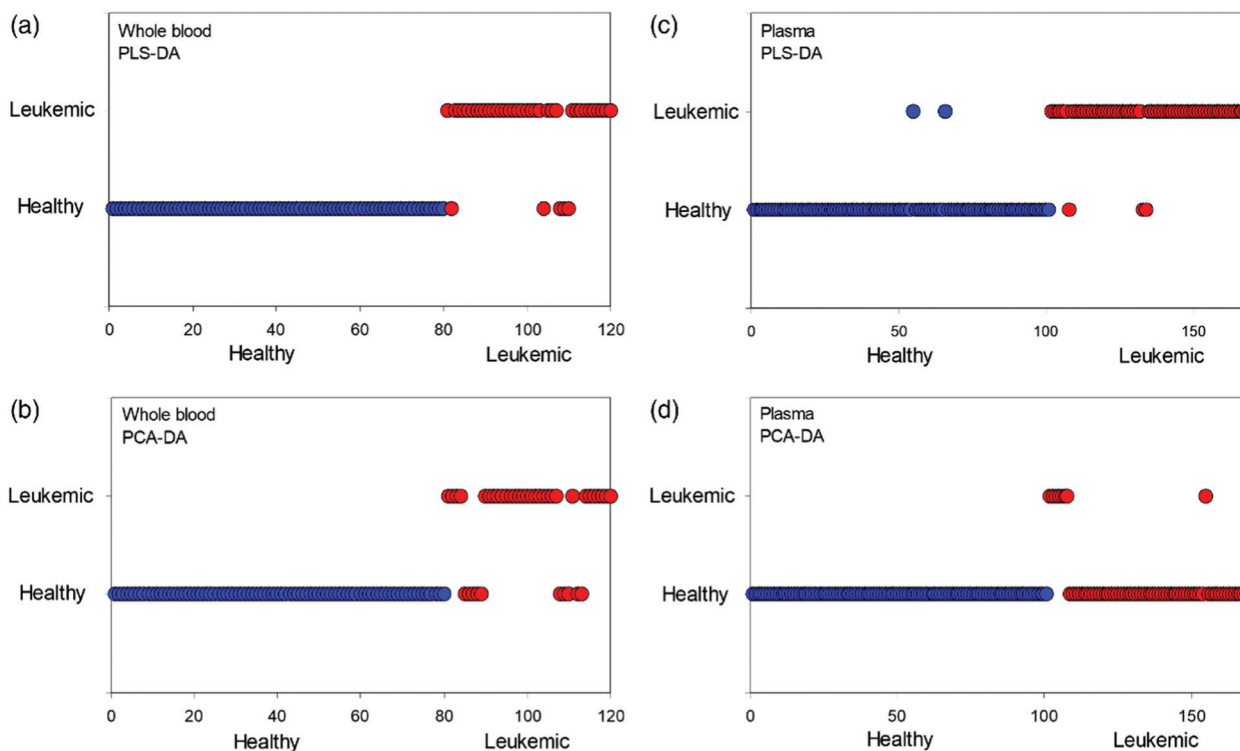


**Fig. 2** Confusion plot with the classifications by healthy group and leukemic group, through the DA, being (a) PLS-DA (whole blood); (b) PCA-DA (whole blood); (c) PLS-DA (plasma); and (d) PCA-DA (plasma). Reprinted with permission from A. M. da Silva, F. S. A. de Siqueira e Oliveira, P. L. de Brito, L. Silveira Jr, Spectral model for diagnosis of acute leukemias in whole blood and plasma through Raman spectroscopy, *J. Biomed. Opt.*, 2018, **23**, 107002. Copyright (2018) SPIE.

tumors) were examined by RS. A PLS-DA classifier for benign *versus* malignant tissues provided 85.7% accuracy at the donor level for external validation. Other binary classification models reached similar levels of success for discerning different types of lymph nodes.<sup>62</sup>

**Oral cancer.** The identification of oral cancer was explored using spontaneous RS and chemometrics. Molecular differences between oral cavity SCC and healthy tissue structures in the tongue were investigated by RS analysis of 44 tongue samples from 21 donors. A non-negative least-squares algorithm was used for fitting to determine the spectral contributions of different chemical classes. Carbohydrate, protein, and amino acid content had the strongest capabilities for discriminating between oral cavity SCC and healthy tissue; a classification model of tumor *versus* healthy tissue was built based on these differences, with results of external validation providing 93% specificity and 100% sensitivity for discrimination.<sup>63</sup> Exfoliated cells from tumor ( $n = 16$ ) and contralateral-normal appearing mucosa ( $n = 16$ ) of oral cancer patients and from healthy tobacco users ( $n = 20$ ) were analyzed *via* PCA-LDA. A model built to separate contralateral-normal and tumor spectra resulted in 74% sensitivity and 73% specificity for identifying normal spectra during LOOCV. A three-class model, including the healthy tobacco users, displayed an average of 70.2% accuracy after LOOCV.<sup>64</sup> Exfoliated cells were again studied in a different and more successful manuscript, this time using both FTIR spectroscopy and RS for discerning normal, pre-cancerous, and cancerous conditions.

PCA-LDA with 10-fold CV of the combined FTIR and RS spectral dataset showed 98% classification accuracy, an improvement upon analysis conducted using only FTIR (85%) or RS (82%) spectral data.<sup>65</sup> Jeng *et al.* investigated 80 tissue samples from the tongue, buccal mucosa, and gingiva of the oral mucosa which represented normal and tumor tissue sites. A PCA-QDA classifier could differentiate the tissues with 90.9% sensitivity and 83.3% specificity after CV, outperforming a PCA-LDA classifier built to achieve the same goal.<sup>66</sup> Lastly, an exploration into both oral and cervical cancer was made using Raman exfoliated cytology. Oral (29 tumor and 15 normal) and cervical (38 tumor and 28 normal) exfoliated cell samples were studied. PCA-LDA with LOSOCV yielded classification efficiencies of 82% and 77% for identifying oral tumor and cervical tumor cells, respectively; these results increased to 86% and 84% classification efficiency for identifying oral tumor and cervical tumor cells at the subject-level.<sup>67</sup> These studies show the importance of which classifier is selected for analysis and the effect of which data is used can have.

**Prostate cancer.** RS analysis using a 1064 nm wavelength laser for excitation was proposed as a method for screening prostate cancer. A classifier based on SVM could predict the Gleason scores (benign, or score of 6, 7, or 8) of 37 prostate tissue specimens of eight donors with 95% classification accuracy after LOSOCV.<sup>68</sup> These results are generally better than those reported further on using SERS.

**Skin cancer.** Feng *et al.* investigated relevant Raman biomarkers for guiding BCC margin resection; data was collected

from skin tissue samples of 30 individuals undergoing Mohs surgery. The data showed that BCC results in different concentrations of nucleus, keratin, collagen, triolein, and ceramide biomolecules compared to normal skin structures. ROC curve analysis and LOSOCV indicated 90% sensitivity and 92% specificity for discriminating between BCC and normal tissue structures.<sup>69</sup> High-wavenumber Raman spectra were collected from 174 excised melanocytic lesions suspicious for melanoma; a PCA-LDA model was developed to distinguish melanomas and non-melanoma, achieving 100% sensitivity and 43.8% specificity after external validation, perhaps indicating this spectral region was not necessarily useful for achieving better diagnostic results.<sup>70</sup> Lastly, non-melanoma skin cancer (BCC and SCC), AK, and normal tissue of 25 subjects were investigated by Raman spectra collected both *in vivo* and *ex vivo*. DA based on Mahalanobis distances was applied for discriminating lesions and normal tissue, achieving 94.1% sensitivity, 93.6% specificity and 93.8% accuracy for classification of the *in vivo* spectra and sensitivity, specificity, and accuracy each of 100% for the *ex vivo* tissue spectra. These results were superior to those achieved using DA performed using Euclidean distances, although no validation scheme was mentioned.<sup>71</sup> Not surprisingly, tissue samples were most commonly used for analyzing skin cancer, providing varying levels of success for classification.

**Thyroid cancer.** Thyroid cancer was studied by a myriad of researchers using spontaneous RS. In one study, FTIR spectroscopy and RS were combined with statistical analysis to distinguish between thyroid adenomas ( $n = 17$ ) and carcinomas ( $n = 15$ ). PCA-LDA with LOOCV showed sensitivities around 62% and 65% and specificities around 70% and 75% for Raman and FTIR spectroscopies, respectively, for distinguishing widely invasive follicular thyroid carcinoma, follicular thyroid adenoma, and normal tissues.<sup>72</sup> In an improvement, Senol *et al.* used an OPLS algorithm to distinguish thyroid tumor and healthy tissue with 81.8% sensitivity and specificity after CV.<sup>73</sup> A different project investigated RS for correctly classifying cell lines which represented benign thyroid cells and various subtypes of thyroid cancer. PCA-LDA, without validation, gave good sensitives (74–85%), specificities (65–93%), and accuracies (71–88%) for identifying thyroid cancer in various binary models.<sup>74</sup> De Oliveira *et al.* obtained Raman hyperspectral images of single cells from benign thyroid ( $n = 127$ ) and classical papillary carcinoma ( $n = 121$ ) nodules. PCA and LDA with CV could identify the cells with 97% diagnostic accuracy, which were the best results obtained recently for identifying the cancer. Further, differences in spectral data collected from cells of follicular adenoma ( $n = 20$ ), follicular carcinoma ( $n = 25$ ), and the follicular variant of papillary carcinoma ( $n = 18$ ) nodules indicated the feasibility of the approach for discrimination of further thyroid cancer subtypes.<sup>75</sup>

## 2.2. Bacterial & viral infections

While there is an abundance of literature published on identifying various cancers using spontaneous RS, research has progressed toward investigating other illnesses, such as infectious diseases with bacterial and viral origins, as well.

Khan *et al.* analyzed blood serum collected from 60 tuberculosis patients and 14 healthy age matched controls using RS.

SVM and PCA with 5-fold CV could diagnose the illness with 92% accuracy, 98% specificity, and 81% sensitivity, illustrating the potential for an early screening mechanism of tuberculosis despite the uneven distribution of sample donors.<sup>76</sup> Another bacterial infection, called *Clostridium difficile* infection (CDI), was also investigated using blood serum. Here, serum was spiked with various concentrations of two different *clostridium* pathogenic factors, (toxin A and toxin B or both). Toxin-spiked serum at various concentrations (1 ng mL<sup>-1</sup>, 1 pg mL<sup>-1</sup>, and 0.1 pg mL<sup>-1</sup>) could be segregated from control serum with 87–100% sensitivity and 77–100% specificity after CV, demonstrating the potential for RS to be used as a sensitive method for detecting clinically relevant concentrations of CDI toxins for diagnostic purposes.<sup>77</sup>

Both hepatitis B and hepatitis C, common viral infections, were studied by different research groups using spontaneous RS. Ditta *et al.* studied blood plasma from hepatitis C infected individuals and healthy donors. The RS data was analyzed using PCA; the differences between spectral features resulted in successful separation of the two groups.<sup>78</sup> In a quantitative study, the hepatitis C infection was explored using RS and a proximity based machine learning technique (PCA-Prox). The PCA-Prox algorithm separated blood serum from 227 infected and healthy donors with accuracy, sensitivity, and specificity levels of 95%, 97%, and 94%, respectively after 5-fold CV. The PCA-Prox algorithm was found to perform better than other classifiers, including KNN, random forest (RF), and SVM.<sup>79</sup> In a large study, Tong *et al.* investigated the potential of RS for diagnosing hepatitis B through analysis of 1000 blood serum samples from healthy and infected donors. The model was built using PCA and SVM; double-blind verification (external validation) of the model's performance showed 87% sensitivity and 92% specificity for the first group and 80% sensitivity and 79% specificity for the second group, showing a potential new method for hepatitis B virus detection.<sup>80</sup> In a smaller study, blood serum from 119 hepatitis B infected and 84 healthy donors were analyzed by RS. SVM with CV gave a diagnostic accuracy of about 98%, an improvement upon the previous study.<sup>81</sup>

The dengue virus infection was studied in several recent manuscripts. RS was used to analyze blood plasma from dengue-infected ( $n = 17$ ) and healthy ( $n = 17$ ) donors. PCA with FDA and LOOCV yielded 97.9% sensitivity and 95.4% specificity for identifying the infection. Further analysis compared healthy donors to patients who scored low on one of the dengue-biomarker tests, but high or medium for two others; the same analysis method was used, resulting in 97.4% sensitivity and 86.2% specificity, fully indicating the method as an unambiguous screening technology.<sup>82</sup> Blood serum of healthy controls was compared to malaria-infected and dengue-infected donors. PCA-LDA could separate malaria, dengue, and healthy control groups with an average accuracy of about 89% after external validation. These results were complemented with mass spectrometry-based analysis, where metabolites assigned to the predominant RS-bands were found to overlap with those trends identified by mass spectrometry.<sup>83</sup> In a related study,

typhoid and dengue infections were analyzed together due to their similarities in symptoms. PCA with LDA and 10-fold CV was applied and could successfully separate the two sets of data, illustrating an interesting potential of RS to separate infections with similar symptoms.<sup>84</sup> Blood, including serum and plasma samples, looks to be the most useful biological fluid for identifying the dengue virus. Of great recent interest, preliminary studies show Raman spectroscopy as being a viable tool for addressing the COVID-19 pandemic, which is caused by the SARS-CoV-2 viral infection.<sup>85</sup> Indeed, Jacobi *et al.* have already begun investigation into mapping the nanostructure of the COVID-19 virus using low-frequency and regular RS and comparing the structure with that of other coronaviruses and viral materials. This work is vital for laying the foundation for future studies into this disastrous disease.<sup>86</sup> Further, Yeh *et al.* propose a microfluidic platform in conjunction with surface enhanced RS as a novel method to track and monitor viral outbreaks, such as the COVID-19 outbreak, in real time.<sup>87</sup> Work which employs surface enhanced RS for diagnostic efforts is discussed further on in Section 3.

### 2.3. Blood disorders & diabetes

Beyond infectious diseases, diagnosis of blood disorders and diabetes have frequently been investigated using spontaneous RS. Research led by da Silva investigated iron deficiency anemia (IDA) and sickle cell disease in comparison to healthy controls. PLS-DA and PCA-DA with LOSOCV were employed; the former resulted in 95.0% and the latter 93.8% diagnostic accuracy.<sup>88</sup> Related, detection of type II diabetes was investigated *via* RS analysis of blood serum from 35 donors. PCA and LDA were used for developing the discrimination method, yielding 96% sensitivity and 99% specificity for classification after LOSOCV.<sup>89</sup>

### 2.4. Kidney, heart, & thyroid diseases

A variety of biological issues associated with the kidney, heart, and thyroid were examined using spontaneous RS. Chen *et al.* explored the ability of RS to classify urine samples from 48 patients with chronic renal failure and from 44 subjects with normal renal function. Five different classifiers were used for distinguishing between the two groups; the best classifier, a grid search SVM, achieved 84.6% diagnostic accuracy after external validation, indicating the potential of the method as a rapid screening tool of urine samples.<sup>90</sup> In an alternate study, different mineral components within kidney stones were investigated. PCA-KNN and PCA-SVM both gave diagnostic accuracies of 96.3% after CV, showing RS can provide support for generating treatment recommendations for patients with kidney stones.<sup>91</sup>

High renin hypertension was explored using serum RS combined with various classification algorithms. Groupings of PCA with SVM, LDA, and KNN plus LOOCV were investigated for generating a prediction algorithm. Both PCA-SVM and PCA-LDA achieved 93.5% diagnostic accuracy whereas the PCA-KNN algorithm demonstrated 89.1% accuracy, indicating the importance of exploring multiple machine learning techniques for achieving optimal results.<sup>92</sup> The same research group continued

on to successfully detect thyroid dysfunction using serum RS and SVM, attaining a diagnostic accuracy of 82.7% for external validation.<sup>93</sup> Du *et al.* explored blood samples from 29 people with normal thyroid function and 38 individuals with hyperthyroidism and 32 with hypothyroidism. PLS-SVM was used for data classification, and the results of external validation indicated discriminatory specificity was 88.8%, sensitivity was 100%, and accuracy was 96.7%, an improvement on the previous study.<sup>94</sup> RS was then used to discriminate between healthy parathyroid tissue and parathyroid adenoma from 18 donors. A PLS-DA model could correctly classify all samples in the calibration and external validation datasets with 100% prediction accuracy. Chief cell adenoma and oxyphil cell adenoma were additionally classified using PLS-DA with 99.8% and 100% accuracy, respectively, after external validation.<sup>95</sup>

### 2.5. Autoimmune & neurodegenerative diseases

Abundant research has been published recently on identifying various autoimmune disorders and neurodegenerative diseases. Fornasaro *et al.* utilized Raman hyperspectral imaging to characterize colon tissues from patients with Celiac disease (CD). Using MCR-ALS, *k*-means cluster analysis, and hierarchical clustering methods, biochemical differences between CD patients and healthy controls were identified which allowed for separation of the two groups. The algorithm was successfully externally validated using samples from patients with Crohn's disease, opening the door for future work to be conducted using an automated algorithm for classification.<sup>96</sup> In a quantitative study, red blood cells (RBCs) from CD patients and healthy donors on a gluten-free diet were analyzed using RS, PLS-DA and ROC curve analysis. Results showed 100% classification accuracy after external validation for correctly predicting the class of a donor.<sup>97</sup>

Ralbovsky *et al.* successfully investigated Alzheimer's disease (AD) and mild cognitive impairment through the analysis of saliva. Using GA and ANN, 100% accuracy was achieved during external validation for differentiating between the three groups.<sup>98</sup> Blood serum was also successfully investigated by the same research group for the identification of AD and other related forms of dementia, achieving high levels of success after external validation.<sup>99,100</sup> Paraskevaidi *et al.* focused on identifying AD and dementia with Lewy bodies in blood plasma. Various binary algorithms were built using SVM to differentiate between healthy controls, early stage AD donors, late stage AD donors, and donors with dementia with Lewy bodies. The classification algorithms achieved an average sensitivity of 81.3% and specificity of 85.7% after CV,<sup>101</sup> suggesting the significance of selecting the best combination of biological sample with statistical analysis method for analysis.

### 2.6. Other diseases

An assortment of other diseases was also investigated using spontaneous RS. Parlatan *et al.* utilized RS for non-invasive diagnosis of endometriosis in a large study (Fig. 3). 94 blood serum samples from healthy and diseased donors were investigated using PCA, KNN, and SVM. The best results were obtained using KNN, achieving 80.5% sensitivity and 89.7% specificity; further verification of the model using unseen data

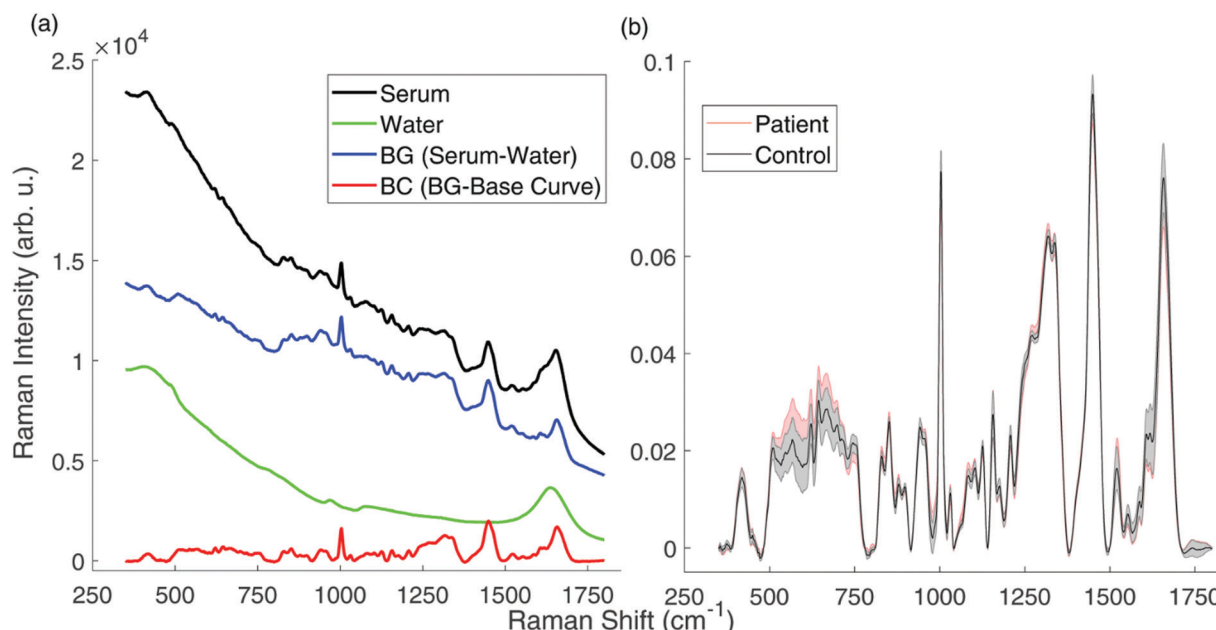


**Fig. 3** (a) Background (BG) and baseline-corrected (BC) Raman spectra of a serum sample. (b) Normalized BC mean Raman spectra of the control and patient groups. Standard deviations of each group were plotted and overlaid as shaded curves. Reprinted with permission from U. Parlata, M. T. Inanc, B. Y. Ozgor, E. Oral, E. Bastu, M. B. Unlu, G. Basar, Raman spectroscopy as a noninvasive diagnostic technique for endometriosis, *Sci. Rep.*, 2019, **9**, 19795. Copyright (2019) Springer Nature.

for external validation yielded sensitivity and specificity values both of 100%.<sup>102</sup> Another research group studied asthma *via* blood serum RS combined with PLS-DA. The classification model attained 100% sensitivity and specificity for correctly predicting the class of a donor in the external validation dataset.<sup>103</sup> Ochronotic and non-ochronotic cartilage was studied by RS for the purpose of monitoring the progress of ochronosis in patients with alkaptonuria, an inherited disorder of tyrosine metabolism. Analysis by PCA-LDA showed effective separation of the groups; further validation of the method is required.<sup>104</sup> In a final study, Sun *et al.* inspected the ability of RS to identify ocular diseases through analysis of tear samples. 69 patients with various ocular diseases (including conjunctivitis, blepharitis, meibomian gland cyst, cataracts, and glaucoma) and 48 healthy donors donated tears; a PLS-SVM algorithm could diagnose ocular diseases with 85.7% accuracy, 100% specificity, and 76.2% sensitivity after external validation, indicating the potential of RS analysis of tears for identifying different ocular diseases.<sup>105</sup>

As these studies so clearly show, the potential of spontaneous RS is vast and can be applied toward investigating any disease which exhibits pathophysiological changes during its progression. Regardless of the biological sample used, the chemometric technique applied, or the disease studied, the promise of the method for medical diagnostics is clear. Spontaneous RS has the advantage of being the most straightforward variation of RS, requiring the least amount of effort to set-up, learn, and understand (that is, in comparison to other methods to be further reviewed). Although the results are promising, more research is necessary to investigate the potential of spontaneous RS for *in vivo* and statistically

significant validated trials, which are crucial for bringing the methodology into clinical settings.

### 3. Surface enhanced Raman spectroscopy

Current efforts in disease diagnostics often focus on the detection of biomarkers which are present at low average concentrations. Many medical diagnostic tests lack either the sensitivity or the specificity, and sometimes both, to detect these crucial biomolecules. In this section, we review the potential of surface enhanced Raman spectroscopy (SERS) to address this need. SERS combines the specificity of Raman spectroscopy with the ability to detect biomolecules present at ultralow concentrations. Typically, the interaction of the laser with the substrate (which are typically nano-sized metal structures) creates a plasmonic light field; molecules that are adsorbed in or near this enhanced field at the surface of the substrate experience enhanced Raman scattering, thus enhancing the produced Raman signal, as well. This enhancement ideally allows for a much more sensitive detection of biomolecules present within a biological sample. This can result in improved discrimination between two similar biological samples, such as those obtained from healthy and diseased donors. While sounding ideal, the SERS method does have a number of potential drawbacks, including the requirement of close contact between the enhancing surface and the sample, limited re-usability of the substrate, and most importantly, potential problems with reproducing the SERS

Published on 30 September 2020. Downloaded by State University of New York at Stony Brook on 10/1/2020 9:16:40 AM.

signal from a substrate.<sup>106</sup> Both the benefits and the limitations of the method are crucial to consider when moving forward toward the goal of creating a successful universal diagnostic method. In this section we discuss recent papers which utilized SERS for detecting various diseases within human biological samples.

### 3.1. Cancer

**Bladder cancer.** Jin *et al.* used SERS to study bladder cancer. Here, tissue from individuals with both luminal ( $n = 24$ ) and basal ( $n = 26$ ) subtypes of bladder cancer were investigated; using PCA-LDA, the two subtypes were classified with 86% accuracy after CV.<sup>107</sup> In a different paper, non-muscle-invasive and muscle-invasive bladder cancer blood serum samples were compared to healthy controls. In a three-group modeling system, PLS-LDA with LOOCV provided an overall diagnostic accuracy of 93.3%. In two different binary models, the same analysis yielded accuracies of 97.8% and 93.2% for considering healthy controls *versus* all bladder cancer groups and for differentiating non-muscle-invasive and muscle-invasive bladder cancer, respectively.<sup>108</sup> Blood serum was also analyzed from 23 low- and 25 high-grade bladder cancer patients as well as 40 healthy volunteers using SERS and SVM. The resultant model gave 96.4% and 95.4% accuracy for separating all bladder cancer samples from normal subjects and for discriminating low- and high-grade bladder cancer serum, respectively, after 10-fold CV.<sup>109</sup> The performance results of these reports are comparable to those conducted using spontaneous RS.

**Breast cancer.** Breast cancer was investigated using SERS by Moisoiu *et al.* in two separate studies. First, urine from 53 breast cancer patients and 22 healthy controls was studied; a PCA-LDA algorithm, with no validation scheme reported, showed the SERS spectra could be differentiated with 81% sensitivity, 95% specificity, and an overall accuracy of 88%, highlighting the ability of the method to be used as a novel screening strategy for breast cancer with no invasive collection procedure.<sup>110</sup> Following this, serum was collected from 253 donors total with either breast, colorectal, lung, ovarian, or oral cancer and healthy controls. PCA-LDA was again used for analysis, this time with 5-fold CV, giving 98% sensitivity and 91% specificity for distinguishing between cancer patients and controls. When comparing each cancer to healthy controls, SERS spectra from each type were correctly assigned with accuracies of 76% for breast cancer, 88% for oral cancer, 86% for colorectal cancer, 80% for ovarian cancer, and 59% for lung cancer after CV, importantly indicating the potential of the developed method for successfully investigating multiple cancers at the same time.<sup>111</sup>

**Colorectal cancer.** Králová *et al.* used SERS for studying colorectal cancer *via* analysis of blood plasma from 15 oncological patients and 15 healthy volunteers. PCA could successfully differentiate between the two groups based on biochemical differences, including those due to tyrosine and adenine.<sup>112</sup> While useful, other studies conducted using spontaneous RS were able to further achieve useful quantitative prediction capabilities useful for diagnostics.

**Gastric cancer.** Investigation of 68 serum samples from gastric cancer patients and healthy controls was conducted by Guo *et al.* Using PCA, biological differences between donors due to nucleic acids, amino acids and carbohydrates was found to be sufficient for separating the two groups.<sup>113</sup> In an alternative study, a detection method based on identifying a modified nucleoside in urine was used for gastric cancer and breast cancer diagnosis. Affinity chromatography was used to purify the modified nucleoside from cancer patient's urine; SERS spectra of the urinary modified nucleoside was collected from 50 gastric cancer patients, 43 breast cancer patients, and 48 healthy volunteers. PCA-LDA with LOOCV could identify each group in three different binary models with an average sensitivity of 80.9% and specificity of 91.3%.<sup>114</sup>

**Head and neck cancers.** Nasopharyngeal cancer was studied by Wu *et al.* *via* SERS analysis of plasma samples from 40 pre-treatment and post-treatment NPC cases as well as 30 healthy volunteers. Binary PCA-LDA models achieved classification with sensitivities of 83.3%, 61.8% and 95.1%, and specificities of 91.2%, 67.4% and 93% for separating pre- and post-treatment samples, post-treatment and normal samples, and pre-treatment and normal samples, respectively, after LOSOCV.<sup>115</sup> Similar results were achieved in a related study using spontaneous RS.

**Leukemia.** Leukemia cell lines were studied using SERS and SVM with leave-one-batch-out CV. Classification yielded sensitivity, specificity, and accuracy levels greater than 99% for differentiating Jurkat, THP-1, and MONO-MAC-6 leukemia cell lysates.<sup>116</sup> Interestingly, these results are comparable to those achieved in several aforementioned studies which employed spontaneous RS.

**Liver cancer.** Liver cancer was exclusively studied using SERS by several different research groups. First, SERS was used to obtain spectra from hepatocellular carcinoma (HCC) tissue; spectra were analyzed using PCA-LDA and LOOCV, giving 93.8% sensitivity and 100% specificity for discriminating between healthy and HCC groups. HCC tissue and adjacent HCC tissue were separated with 79.2% sensitivity and 93.8% specificity.<sup>117</sup> In one large and successful study, serum protein samples were obtained from 104 liver cancer patients and 100 NPC patients as well as 95 healthy volunteers. PLS with SVM could classify the three groups with 95.1% and 90.7% accuracy using training and unknown testing (external validation) datasets, respectively. Further, PLS was found to be a better dimensionality reduction method than PCA.<sup>118</sup> In an even larger combination study, SERS spectra of serum from 304 normal individuals, 333 patients with hepatopathy, and 99 patients with esophageal cancer were studied. OPLS-DA with ROC curve analysis and 10-fold CV could differentiate between the various groups with AUC values all greater than 0.97, indicating excellent classification.<sup>119</sup> Zhang *et al.* studied cancerous and normal liver tissue slices from 56 patients with liver cancer; PCA-LDA was used for classification, giving 100% sensitivity and specificity, each, after ROC curve analysis. No additional validation was reported.<sup>120</sup> Based on the successful results of all reports, the efficacy of SERS for detecting liver cancer is unquestionable.

**Lung cancer.** Lung cancer was heavily studied using SERS. Qian *et al.* analyzed saliva samples from 127 healthy and lung

cancer patients; SVM and RF were used for generating prediction algorithms. Using SVM with LOOCV, 95.1% sensitivity and 100% specificity was achieved. RF with LOOCV reached 96.7% sensitivity and 100% specificity, indicating both statistical analysis methods were successful for identifying the cancer.<sup>121</sup> Zhang *et al.* used PCA-LDA to interrogate SERS serum spectra of 50 lung cancer donors and 50 healthy controls. With ROC curve analysis, 100% sensitivity and 90% specificity was accomplished.<sup>122</sup> In further research by the same group, tissue slices from a smaller set of donors was studied using PCA-LDA and ROC curve analysis, resulting in 95.7% sensitivity and specificity, each, of the method, comparable to their study performed using serum.<sup>123</sup> Interestingly, validation was not reported in either study. Cao *et al.* developed a serum-based SERS test for diagnosing non-small cell lung cancer. Here, PCA could distinguish between different types of NSCLC due to intrinsic differences in biochemical composition.<sup>124</sup> NSCLC was also studied in a different project *via* exosomes from normal and NSCLC cells. The unique peaks of cancerous exosomes were extracted using PCA, allowing for decent separation of the two groups.<sup>125</sup> In a quantitative study by Liu *et al.*, human serum from normal individuals ( $n = 82$ ) and individuals with lung adenocarcinoma ( $n = 108$ ) was analyzed using SERS (Fig. 4). OPLS-DA could separate the two groups with 97.6% specificity and 98.1% sensitivity after LOSOCV. Staging lung adenocarcinoma was also successful; accuracies of screening for stage I, stage II, and stage III/IV reached 84.3%, 93.3%, and 86.5%, respectively.<sup>126</sup> Malignant pleural effusion (PE) was studied by the same group *via* SERS analysis of 83 PE samples, including 32 benign PE and 51 malignant PE. OPLS-DA was again used, providing 92.2% sensitivity and 93.8% specificity for diagnoses based on LOOCV.<sup>127</sup> Although a variety of biological samples were analyzed and machine learning methods were used, the results of SERS analysis for identifying lung cancer are generally comparable to each other, demonstrating extreme strength and utility of the method; notably, several studies

which did not report validation require further investigation to verify the true strength of the method.

**Oral cancer.** Recently, two different groups investigated the diagnosis of oral cancer using SERS. One group analyzed serum samples from 135 oral SCC patients at various tumor stages and histologic grades; PCA with LDA could accurately detect oral SCC based on tumor size, lymph node metastasis, and histologic grades all with accuracies of detection greater than 85% after LOOCV.<sup>128</sup> In the second smaller study, oral tissue samples from 37 patients were examined. Oral tissues consisting of oral SCC, verrucous carcinoma, premalignant leukoplakia, and disease-free conditions were classified with an accuracy of 97.2% using PCA-DA with CV. Three grades of oral SCC tumors were further classified with 97.8% accuracy, indicating the potential of SERS for use as a point-of-care tool.<sup>129</sup> These two reports are generally more successful than the studies conducted using spontaneous RS.

**Ovarian cancer.** Ovarian cancer was exclusively analyzed using SERS technology in the last two years. SERS was first used to evaluate the potential of haptoglobin in ovarian cyst fluid as a potential diagnostic biomarker for epithelial ovarian cancers. In comparison with histology, measurements of haptoglobin resulted in 94% sensitivity and 91% specificity of detection after CV. Logistic regression with ROC curve analysis gave an AUC of 0.966.<sup>130</sup> Zermeno-Nava *et al.* used SERS to determine the sialic acid levels in saliva for the purpose of comparing benign tumor and ovarian cancer patients. ROC curve analysis established a cut-off value of sialic acid ( $15.5 \text{ mg dL}^{-1}$ ), which yielded 80% sensitivity and 100% specificity for distinguishing between the two cases. No validation was reported.<sup>131</sup> In a comparison study, Paraskevaidi *et al.* used both SERS and spontaneous RS to probe blood plasma samples from 27 patients with ovarian cancer, including 17 early cases, and 28 donors with benign gynecological conditions (Fig. 5). Analysis of SERS data by SVM with CV could detect ovarian cancer with 87% sensitivity and 89%

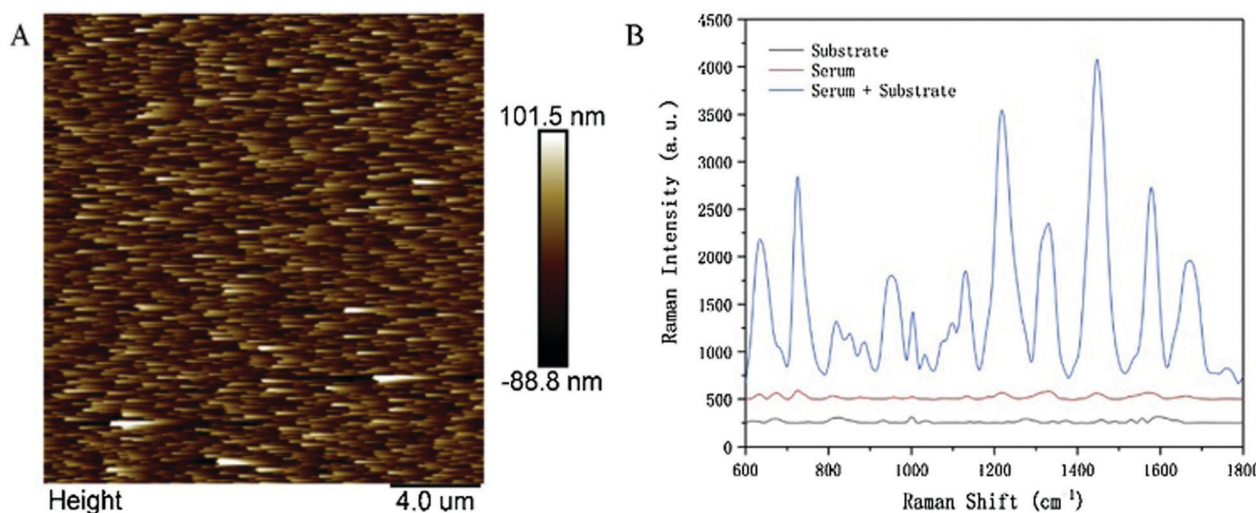
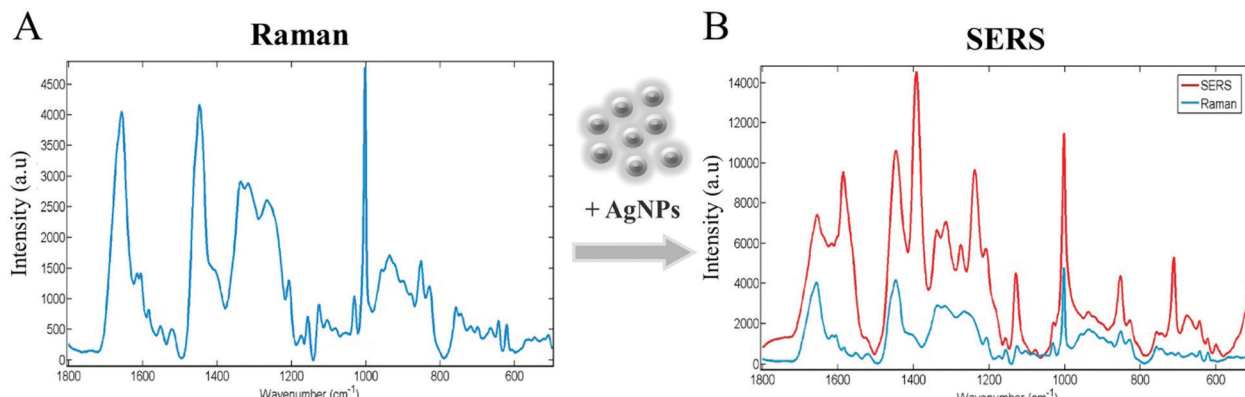


Fig. 4 Characterization of Ag nanorods wrapped with  $\text{Al}_2\text{O}_3$  layer. (A) AFM image of the prepared substrate. (B) Raman spectra of Ag nanorods wrapped with  $\text{Al}_2\text{O}_3$  layer, serum, and serum with the substrate. Reprinted with permission from K. Liu, S. Jin, Z. Song, L. Jiang, L. Ma, Z. Zhang, Label-free surface-enhanced Raman spectroscopy of serum based on multivariate statistical analysis for the diagnosis and staging of lung adenocarcinoma, *Vib. Spectrosc.*, 2019, **100**, 177–184. Copyright (2019) Elsevier B.V.



**Fig. 5** Enhancement effect of SERS after the addition of silver nanoparticles (AgNPs) in blood samples. Reprinted with permission from M. Paraskevaidi, K. M. Ashton, H. F. Stringfellow, N. J. Wood, Raman spectroscopic techniques to detect ovarian cancer biomarkers in blood plasma, *Talanta*, 2018, **189**, 281–288. Copyright (2018) Elsevier B.V.

specificity; early ovarian cancer was identified with 80% sensitivity and 94% specificity. Interestingly, these results were not an improvement compared to spontaneous RS, which could detect ovarian cancer with 94% sensitivity and 96% specificity and early ovarian cancer with 93% sensitivity and 97% specificity.<sup>132</sup> It should be noted these studies show a wide variety of biological fluids are useful for identifying ovarian cancer with similar levels of success.

**Pancreatic cancer.** Two reports were made on studying pancreatic cancer using SERS. Li *et al.* used ROC curve analysis to show that a migration inhibitor factor SERS-based immunoassay could discriminate between 71 pancreatic cancer patients and 32 healthy individuals as well as distinguish metastasized tumors from metastasis-free tumors, and Tumor Node Metastasis P1–2 stages from the P3 stage with 95.7% discriminatory sensitivity; however, no validation was reported.<sup>133</sup> In the second study, exosomes purified from normal and pancreatic cancer cell lines were studied via SERS and PCA-FDA; the origin of the exosomes could be identified with 90% accuracy after external validation. Interestingly, the cell-line trained model could also differentiate serum-purified exosomes with 87% and 90% accuracy after external validation for healthy control and prostate cancer samples, respectively, depicting the universality of the technique.<sup>134</sup>

**Prostate cancer.** The last cancer recently studied using SERS was prostate cancer. In one publication, PCA and ROC curve analysis could score the risk of developing prostate cancer through analysis of urine with 87% sensitivity and 90% specificity after external validation and an AUC of 0.84, providing a risk stratification approach to diagnosing prostate cancer.<sup>135</sup> Stefancu *et al.* combined SERS serum spectra with serum prostate-specific antigen levels of prostate cancer and nonmalignant pathologies to build a discriminatory algorithm using PCA-LDA. The model yielded 94% accuracy for discriminating between 30 cancerous and 24 control serum samples, though no validation scheme was mentioned.<sup>136</sup> SERS with PCA-LDA was used in a large study to evaluate early biochemical recurrence after radical prostatectomy. 306 preoperative plasma spectra from 102 patients were collected and a comparison was made between those who developed early biochemical recurrence and those who remained biochemical

recurrence-free. Using PCA-LDA with LOOCV, the model revealed 65.8% sensitivity, 87.5% specificity, and 79.4% accuracy, suggesting a novel method for predicting early biochemical recurrence in prostate cancer.<sup>137</sup>

### 3.2. Bacterial, parasitic, & viral infections

Outside of cancer, infections from various sources are commonly studied using SERS. The bacterial infection methicillin-resistant *Staphylococcus aureus* (MRSA) was investigated in comparison to methicillin-sensitive *Staphylococcus aureus* (MSSA); 52 MSSA isolates and 215 MRSA isolates from clinical samples were discriminated by PLS-DA with 10-fold CV, achieving almost 100% diagnostic accuracy, indicating SERS as a potential tool for studying antibiotic-resistance.<sup>138</sup> Pérez *et al.* investigated Chagas disease, a parasitic infectious disease, in blood serum samples. A total of 110 samples were collected from healthy donors and infected donors, who were split into asymptomatic and symptomatic groups. PCA and LDA was used for analysis, generating 96.3% accuracy for correctly classifying the samples into one of the three groups after external validation.<sup>139</sup> In a different study, sialic acid levels in saliva among 93 total periodontitis-affected, gingivitis, and control patients were measured using SERS. ROC curve analysis was used to determine the optimum threshold of sialic acid concentration for discrimination; threshold concentrations were found to be 5.98, 7.32, and 17.12 mg dL<sup>-1</sup> for control, gingivitis, and periodontitis patients, respectively, confirming the possibility of SERS as a diagnostic tool for frequent bacteria-causing oral diseases; further validation of the method is necessary.<sup>140</sup> A diagnostic assay for identifying Ebola and malaria was developed using SERS to detect antigens from each within a single blood sample. 190 clinical samples collected from the 2014 West African Ebola outbreak were studied in addition to 163 malaria positive and 233 negative controls. After ROC curve analysis, Ebola was detected with 90.0% sensitivity and 97.9% specificity and malaria with 100% sensitivity and 99.6% specificity, showcasing SERS as an important tool for outbreak detection in low resource areas. Notably, validation of the method will be required to move it forward.<sup>141</sup> The analysis of various

biological samples using SERS is clearly useful for identifying a variety of different infectious diseases, regardless of their origin.

### 3.3. Kidney & heart diseases

SERS was used in one study to investigate the diagnosis of chronic kidney diseases. SERS spectra were collected from 50 normal and 60 afflicted individuals; PCA with LDA was used for statistical analysis, showing 100% sensitivity and specificity for classification after external validation.<sup>142</sup> In a different study, a prospective diagnostic method for coronary heart disease was investigated using SERS spectra of urine samples. Urine from 87 patients with the disease, including those with percutaneous coronary intervention (PCI) before operation and those without PCI, and 20 healthy controls was measured. PCA-LDA and LOSOCV could correctly classify the SERS spectra with 90% sensitivity and 78.9% specificity, showcasing the ability of the method to detect the disease with minimal invasiveness.<sup>143</sup>

### 3.4. Autoimmune & neurodegenerative diseases

Analysis of the autoimmune disorder Sjogren's syndrome (SjS) was studied by Stefanu *et al.* Here, saliva and blood serum from 21 healthy donors and 29 SjS patients was collected and analyzed using SERS. PCA-LDA models with LOOCV built using each body fluid yielded classification accuracies of 94% for saliva and 98% for serum, suggesting SERS analysis as a potential novel point-of-care diagnostic method.<sup>144</sup> The neurodegenerative disorder, amyotrophic lateral sclerosis (ALS), was explored *via* SERS analysis of blood plasma from 138 sporadic ALS cases (Fig. 6). PCA, ROC curve, and CV analysis showed spectral differences between the short-duration group and long-duration group of sporadic ALS cases, which could be classified with an AUC of 0.972.<sup>145</sup>

Two studies were published which used SERS for diagnosing AD. The first study focused on optimizing a protocol for analyzing blood serum of AD and healthy control donors. PCA and LDA were used for statistical analysis; LOOCV gave diagnostic accuracy, precision, and specificity values of 83%, 86%, and 86%. A direct comparison of the SERS spectra was

made to hippocampus degeneration, indicating a promising potential instrument for monitoring AD progression.<sup>146</sup> Ryzhikova *et al.* also used SERS for studying blood serum, here of 48 AD, healthy controls, and donors with other forms of dementia. ANN achieved diagnostic accuracies of 96% for differentiating AD and healthy controls and 98% for identifying AD, healthy control, and donors with other forms of dementia in a tertiary model after external validation.<sup>147</sup> Interestingly, these results are comparable to those which were achieved using spontaneous RS for AD detection.

### 3.5. Other diseases

An assortment of other diseases has additionally been studied using SERS analysis of various biological samples. Kim *et al.* used SERS to investigate amniotic fluids of individuals with subclinical intra-amniotic infection and preterm delivery; these prenatal diseases could be identified using PCA-SVM with greater than 92% clinical sensitivity and specificity; unfortunately, no validation was reported.<sup>148</sup> Knee osteoarthritis was studied *via* SERS analysis of synovial fluid combined with PCA-LDA and LOSOCV. The classification algorithm provided a diagnostic accuracy of 91% for distinguishing between low-grade and high-grade osteoarthritis. Resonant RS data was also collected from the same samples, reaching a diagnostic accuracy of 74%. Interestingly, combining the two sets of spectral data gave a classification accuracy of 100%.<sup>149</sup> SERS spectra of saliva from 26 children with asthma and 18 healthy children was investigated using PCA-LDA with LOOCV; the method resulted in a sensitivity of 85%, specificity of 82%, and accuracy of 84% for separating asthmatic saliva from control saliva.<sup>150</sup> Lin *et al.* performed research on type II diabetes using SERS of blood plasma from 35 diabetic and 45 healthy individuals. PCA and LDA could identify diabetic SERS spectra with a specificity of 100% and sensitivity of 80% during external validation. ROC curve analysis showed an optimal AUC of 1.00,<sup>151</sup> which is comparable to the study performed using spontaneous RS. Lastly, causative pathogens for the two most common sexually transmitted diseases, *Chlamydia trachomatis* (elementary bodies, EB) and *Neisseria gonorrhoeae*, were studied. SERS signatures were collected *in vitro* for both and showed obvious differences between the two.

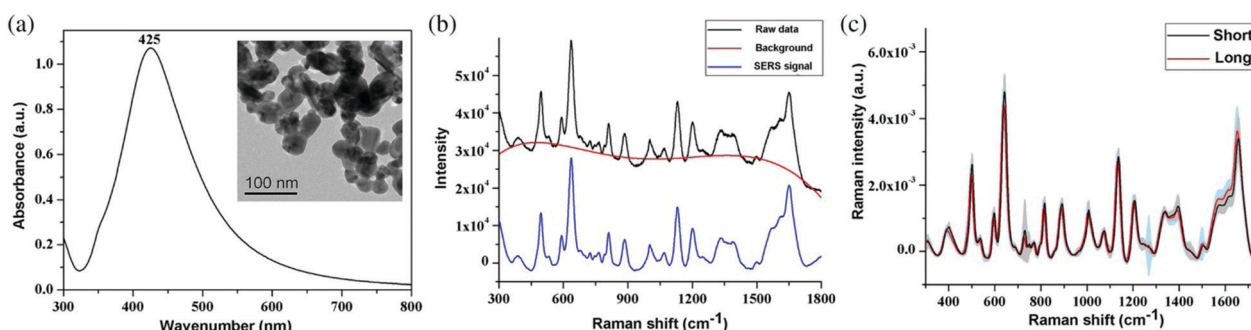


**Fig. 6** The spectral characteristics of blood plasma analyzed using SERS. (a) The UV/visible absorption curve and micrograph of silver colloid obtained using an electron microscope. The absorption maximum is located at 425 nm. (b) Typical raw spectra and the effect of autofluorescence subtraction applied during SERS data preprocessing. (c) Comparison of the mean spectrum of the short-duration group (black line,  $n = 62$ ) vs. that of the long-duration group (red line,  $n = 76$ ). The shaded areas represent the standard deviations of the means. Reprinted with permission from Q.-J. Zhang, Y. Chen, X.-H. Zou, W. Hu, X.-L. Lin, S.-Y. Feng, F. Chen, L.-Q. Xu, W.-J. Chen, N. Wang, Prognostic analysis of amyotrophic lateral sclerosis based on clinical features and plasma surface-enhanced Raman spectroscopy, *J. Biophotonics*, 2019, **12**(8), e201900012. Copyright (2019) John Wiley & Sons, Ltd.

PLS-DA could discriminate SERS spectra of *Chlamydia trachomatis* from spectra of avidin and human serum albumin proteins with 99%/97% sensitivity and 98%/96% specificity for Au/Ag substrates after CV.<sup>152</sup>

Using SERS for examining a wide variety of diseases is shown here to be just as successful, if not more so in some cases, than the previously reviewed spontaneous RS studies. While more time is required to prepare the substrates used in SERS analysis, the potential of the method for achieving positive results with greater sensitivity is apparent. It is necessary to contemplate both the benefits and the limitations of the technique as effort is made toward achieving a singular universal diagnostic method based on Raman spectroscopy.

## 4. Other variations of Raman spectroscopy

While SERS and spontaneous RS account for the majority of the research articles written in the past two years, there still remain other variations of RS which were used for the similar purpose of developing novel medical diagnostic methods. These techniques are briefly described herein and are organized by the specific approach used.

### 4.1. Deep-ultraviolet Raman spectroscopy

Deep-ultraviolet Raman spectroscopy (DUVRS) was used in two recent studies. DUVRS utilizes an excitation wavelength in the deep ultraviolet range of light which increases the inelastic scattering produced by biological samples composed of aromatic amino acids and nucleic acids due to their absorption of light in the same range. Generally, less fluorescence interference is also known to occur at wavelengths shorter than 250 nm, thus resulting in a Raman spectrum with an improved signal-to-noise ratio.

In one study, DUVRS was used to investigate the spores of eight different fungal species implicated in respiratory diseases. PCA-LDA generated classification models built at the genus, species, and strain levels. After leave-one-batch-out CV, an accuracy of 97.5% at the genus level was achieved, the four different *Aspergillus* species were classified with 100% accuracy, and the three different *Aspergillus fumigatus* strains were classified with 89.4% accuracy, demonstrating DUVRS as an innovative approach for fast identification of fungal spores related to respiratory diseases.<sup>153</sup> Ralbovsky *et al.* similarly used DUVRS for diagnostic purposes, showing in a proof-of-concept study that both cancerous and control brain tissue and normal and cancerous prostate cells could be easily discriminated, setting the stage for a quantitative study to be performed in the future.<sup>154</sup>

### 4.2. Raman spectroscopy combined with optical tweezers

The combination of RS with optical tweezers is a powerful tool used for characterizing and evaluating cells in a non-invasive and sterile way. The cells are captured by optical force, preventing random motion. Further, the laser tweezer RS (LTRS) system can collect Raman spectra from single living cells without interference of substrates or their liquid environment.

LTRS was used by Liu *et al.* to examine colon cancer cells with single base mutations in the KRAS gene. The different cell lines include DKS-8 (KRAS wild-type [WT]), DLD-1 (KRAS mutant-type [MT]), HKE-3 (KRAS WT), and HCT-116 (KRAS MT). When using PCA-LDA statistical analysis, DKS-8 and DLD-1 cells were classified with 97.5% accuracy, HKE-3 and HCT-116 cells were classified with 97% accuracy, and classification efficiency of WT *versus* MT cells reached 81.2%. Although no validation was reported, these results are comparable to similar studies which used spontaneous RS and SERS, thus providing promising results for further development of a successful detection method of circulating tumor cells in a liquid biopsy.<sup>155</sup> Extracellular vesicles (EV) released by mammalian cells was explored in a different paper as a potential prostate cancer biomarker. LTRS was used to collect the Raman signatures of four different EV samples which consisted of RBC- and platelet-derived EVs of healthy and prostate cancer cell lines (Fig. 7). PCA could easily separate and classify the groups, setting the stage for future work to use EVs for monitoring prostate cancer.<sup>156</sup>

RBCs were explored to identify β-thalassemia, an inherited blood disorder, using a LTRS system. Raman spectra of RBCs from 33 patients with β-thalassemia-major, 49 with β-thalassemia-minor, and 65 healthy controls were collected. Once again, it was found that PCA could successfully distinguish between RBCs of β-thalassemia-major patients and healthy controls. Further improvement to the recognition of β-thalassemia-minor is required.<sup>157</sup> In a final study utilizing LTRS, RBCs were again analyzed, this time for detecting type II diabetes. An algorithm built using PCA-LDA could differentiate between RBCs of healthy donors and those with diabetes with 100% sensitivity and 90% specificity after external validation,<sup>158</sup> which is similar to results obtained using both spontaneous RS and SERS for identifying type II diabetes. The LTRS system provides a great capacity for studying cells for diagnostic purposes, but it should be noted it does not apply for studying other biological samples, thus making it difficult for universal medical diagnostics.

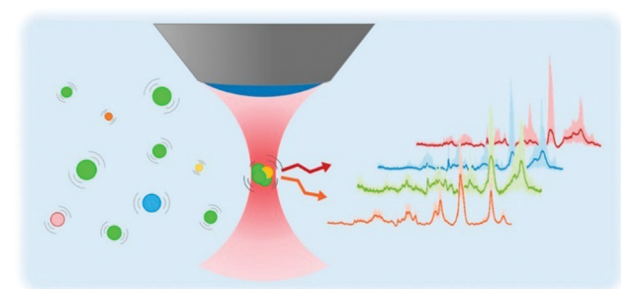


Fig. 7 Schematic depiction of Raman optical tweezer system used to obtain the Raman signatures of four different extracellular vesicle samples. Adopted with permission from W. Lee, A. Nanou, L. Rikkert, F. A. W. Coumans, C. Otto, L. W. M. M. Terstappen, H. L. Offerhaus, Label-free prostate cancer detection by characterization of extracellular vesicles using Raman spectroscopy, *Anal. Chem.*, 2018, **90**(19), 11290–11296. Copyright (2018) American Chemical Society.

#### 4.3. Shifted-excitation Raman difference spectroscopy and dual excitation Raman spectroscopy

Shifted-excitation Raman difference spectroscopy (SERDS) was used in one study to classify 8 breast tissue samples as healthy, fibroadenoma, or invasive carcinoma. SERDS involves the collection of spectra using two slightly different excitation wavelengths; when the difference of the two spectra is taken, the contribution of fluorescence is ideally removed, resulting in better interpretability of the obtained spectra. Here, the excitation wavelengths used were 784 nm and 785 nm. The differences in spectra were examined using PCA and LDA, which gave excellent classification after LOOCV. Specifically, invasive breast carcinoma and the absence of invasive breast carcinoma were identified with 99.2% and 90.4% sensitivity and specificity, respectively. Tumor tissue in tumor-containing tissue could be recognized with 100% sensitivity and the absence of tumor in the no-tumor containing tissue was recognized with 100% specificity. This study shows SERDS has a strong potential for supporting histopathological diagnoses of various breast pathologies,<sup>159</sup> with results comparable to those obtained using spontaneous RS.

Two different studies employed dual excitation RS for the identification of prostate cancer in biological samples. Pinto *et al.* utilized a dual-wavelength laser source (680 nm and 785 nm excitation) for collecting spectra from 20 whole prostates following prostatectomy. Dual excitation captures both the fingerprint and the high wavenumber region of Raman spectral data at the same time. The obtained spectral data from the prostate and the extra prostatic tissue was distinguished with 91% accuracy, 90.5% sensitivity, and 96% specificity after ROC curve analysis with external validation. *In vivo* spectra were also collected from four patients, showing similarities to the spectra collected *ex vivo*, indicating the potential for future expansion of the work.<sup>160</sup> In a second study, dual excitation wavelength RS (671 nm and 785 nm excitation) was used to collect data simultaneously from fingerprint and high wavenumber Raman spectra. 18 prostate slices obtained post-prostatectomy were analyzed; SVM with LOOCV and ROC curve analysis could differentiate between normal and cancerous spectra with an AUC of 0.91 when data from both excitation wavelengths was combined, which was an improvement upon results obtained from each considered separately.<sup>161</sup> Interestingly, these methods show great potential for studying two different types of cancer with similar levels of success as those obtained by means of more well-used variations of RS; supplementary research would be necessary to understand any further benefit of the methods toward investigating other diseases.

#### 4.4. Fiber optic probes and handheld instruments

Raman spectroscopic systems which employ the use of fiber-optic probes are beginning to gain popularity for medical diagnostic studies. The use of probe systems is a transition to the ultimate goal of reaching *in vivo* detection of various maladies. Typically, the system consists of the laser source, the handheld fiber-optic Raman probe itself, a compact spectrometer, and a detector. The entire system is small, portable, and

easy to use within clinical settings. The fiber-optic probes are less expensive than benchtop Raman spectrometers, take up less space, and most importantly, can be used intra-operatively, preventing the need for any additional testing or surgeries to obtain biological samples. The analysis time is short but still sufficient for capturing useful biochemical information about a sample.

Fiber-optic probes have been employed in a variety of research endeavors for medical diagnostic purposes. In two different studies, Chen *et al.* investigated their use for identifying bladder cancer. First, a low-resolution fiber-optic Raman sensing system (Fig. 8) was used to evaluate a total of 32 different *ex vivo* bladder specimens which were considered either normal bladder tissues, low-grade bladder tumors, or high-grade bladder tumors. PCA-ANN with CV successfully discriminated the groups with an overall accuracy of 93.1% and an average sensitivity and specificity of 91.3% and 97.3%, respectively.<sup>162</sup> In a follow-up study, a variety of experimental conditions as well as chemometric techniques were considered for optimizing the method for clinical applications. Here, spectral data was collected from 42 bladder tissue specimens from 10 patients who were either healthy or had high- or low-grade bladder cancer. It was found that increasing the integration time had the greatest improvement on prediction accuracy. The best results were obtained using PCA-ANN with a laser power of 150 mW and integration time of five seconds; the overall accuracy of the tertiary classification system under these parameters was 95.4% with an average sensitivity of 94.9% and specificity of 97.6% after CV.<sup>163</sup> This study further confirms the ability of the low-resolution Raman fiber-optic system for identifying bladder cancer pathologies with similar, if not better, levels of success as SERS and spontaneous RS.

Li *et al.* used their own fiber-optic RS system to collect data from 16 breast tissue samples from healthy controls and individuals with breast cancer. A novel algorithm of entropy weighted local-hyperplane KNN was used for identifying spectra, yielding 92.3% accuracy, 93.8% sensitivity, and 87.8% specificity during randomized grouping CV. These results were an improvement over KNN alone as well as the adaptive weighted *k*-local hyperplane algorithm.<sup>164</sup>

A custom-made microprobe was used for collecting *in vivo* Raman spectra from 13 cancerous and 17 healthy lung tissues for the detection of lung cancer. A novel variational classifier based on SVM with hierarchical CV yielded 93% accuracy for differentiation between the samples.<sup>165</sup>

NPC was also studied *via* fiber-optic RS. In one study, *in vivo* fingerprint and high wavenumber region spectra were collected from 14 NPC patients and 48 healthy subjects during nasopharyngeal endoscopic examinations. GA-PLS-LDA was used for classifying the spectra; after LOSOCV, the algorithm achieved 98.2% diagnostic accuracy, 93.3% sensitivity, and 100% specificity. The research suggests a strong potential for the fiber-optic system to improve real-time *in vivo* detection of NPC over other methods such as SERS.<sup>166</sup> In a slightly alternative approach, Desroches *et al.* investigated the high wavenumber region of Raman spectral data using a core needle biopsy probe

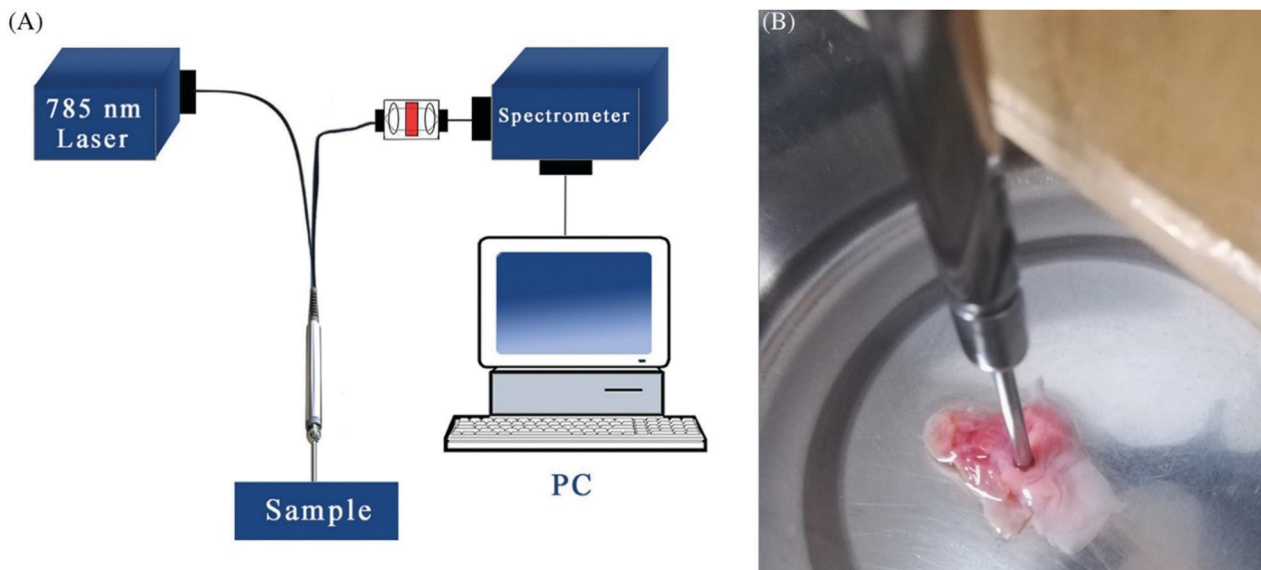


**Fig. 8** (A) The low-resolution fiber-optic Raman sensing system used in this study (an additional long-pass filter stage is added before the collected signal goes into the spectrometer); (B) probe placement during measurement. Reprinted with permission from H. Chen, X. Li, N. Broderick, Y. Liu, Y. Zhou, J. Han, W. Xu, Identification and characterization of bladder cancer by low-resolution fiber-optic Raman spectroscopy, *J. Biophotonics*, 2018, **11**(9), e201800016. Copyright (2018) John Wiley & Sons, Ltd.

system for detection of human dense cancer of brain tissue *in situ* during surgery. The method achieved 80% sensitivity and 90% specificity using SVM with LOOCV.<sup>167</sup>

Prostate cancer was investigated using a handheld contact RS probe system. Here, 32 post-prostatectomy specimens were analyzed; spectra were collected from areas characterized by tissue type (extraprostatic or prostatic), tissue malignancy (benign or malignant), cancer grade (grade groups I–V), and tissue glandular level. Neural networks with LOOCV and ROC curve analysis was used for determining the diagnostic abilities of the RS method. Extraprostatic and prostatic tissue were distinguished with 82% sensitivity and 83% specificity; benign and malignant tissue with 87% sensitivity and 86% specificity; and benign *versus* each grade group were compared in several binary models, achieving an average sensitivity of 81.8% and specificity of 85.2%, depicting the potential of the method for allowing RS studies to move into clinical settings for identifying prostate cancer.<sup>168</sup> The same group of researchers showed in a previous study they could also use their handheld contact probe for accomplishing *in vivo* detection of cancer cells within the brain. Using the probe, normal brain, dense cancer, and normal brain invaded by cancer cells were differentiated with 93% sensitivity 91% specificity using a boosted trees algorithm with CV.<sup>169</sup>

Feng *et al.* investigated the use of a fiber-optic RS system for identifying biophysical markers for skin cancer diagnosis. An inverse biophysical skin cancer model was developed to better understand the biophysical changes which occur and allow for diagnoses. Spectra were collected *in vivo* from 65 patients who were diagnosed with either malignant melanoma, dysplastic nevi, BCC, SCC, or AK. A logistic regression model with LOSOCV identified diagnostically relevant model components.

Interestingly, the developed biophysical model could capture the diagnostic power of the previously developed statistical classification model while additionally providing information about the skin's biophysical composition.<sup>170</sup> In a different study, a non-classical logic called paraconsistent logic was used to differentiate between various cutaneous tissue samples analyzed by RS. Spectra from four histopathological groups, including 115 spectra of BCC, 21 of SCC, 57 of actinic keratosis (AK), and 30 of normal skin were collected. The normal skin group was compared to the group of non-melanoma cancer lesions (BCC + SCC) and the AK tumor lesion; the paraconsistent algorithm achieved 75.8% efficiency after CV, which was superior to the classification system built using PCA-DA.<sup>171</sup>

Two different articles focused on investigating tongue SCC using fiber optic RS. Yu *et al.* collected spectral data from tumorous and non-tumorous tissue of 12 patients who had undergone a surgical resection due to tongue SCC (Fig. 9). Deep convolutional neural networks (CNN) could classify the data with 99.3% sensitivity and 94.4% specificity after 5-fold CV.<sup>172</sup> Similarly, Yan *et al.* also used CNN to discriminate tongue SCC from non-tumorous tissue. Here, the model yielded 99.1% sensitivity and 95.4% specificity; despite no validation reported, the study indicates the strong potential of CNN with fiber-optic RS to evaluate tongue SCC intraoperatively.<sup>173</sup> Interestingly, tongue cancer was not studied using other variations of RS, suggesting the advantage of fiber-optic RS probes for studying a less frequently examined cancer.

Handheld Raman spectrometers were likewise investigated for a variety of diagnostic purposes. Handheld spectrometers, while similarly advantageous to probes, have different features. The handheld instruments can also make *in vivo* diagnoses, are also smaller and less cumbersome than a desktop instrument

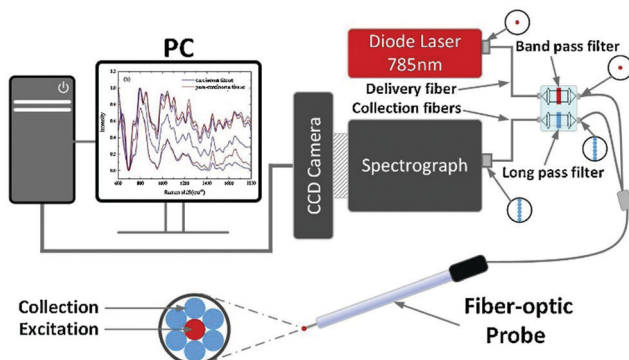


**Fig. 9** Schematic description of fiber optic Raman spectroscopy system. Reprinted with permission from M. Yu, H. Yan, J. Xia, L. Zhu, T. Zhang, Z. Zhu, X. Lou, G. Sun, M. Dong, Deep convolutional neural networks for tongue squamous cell carcinoma classification using Raman spectroscopy, *Photodiagn. Photodyn. Ther.*, 2019, **26**, 430–435. Copyright (2019) Elsevier B.V.

and are less expensive. Handheld Raman spectrometers function more under the idea of “point-and-shoot”, making them incredibly user-friendly and plausible for both clinical and at-home measurements. While the handheld instrument is much smaller and more cost-effective than a benchtop instrument, the resolution is not always comparable. However, the continuous improvement of these instruments and their specifications has allowed for some recent successful studies.

Guevara *et al.* used a handheld Raman spectrometer for investigating type II diabetes. Here, *in vivo* spectra were collected from afflicted individuals and healthy controls from four different sites (ear lobe, inner arm, thumb nail, and median cubital vein). ANN with CV could discriminate between the groups with 88.9–90.9% accuracy. PCA with SVM with CV did not perform as well, achieving only 76–82.5% diagnostic accuracy. With the success of the ANN algorithm, the method showed to be a promising tool for non-invasive and automated detection of type II diabetes.<sup>174</sup>

A portable and cost-effective spectroscopic system (Fig. 10) was employed by Khristoforova *et al.* to study skin cancer. Skin tumors including malignant melanoma, BCC and various benign neoplasms were studied *in vivo*; in addition, autofluorescence spectra were also collected. PLS-DA analysis with LOOCV of both Raman and autofluorescence spectra gave specificity and sensitivity levels between 78.9% and 100% for identifying the various pathologies.<sup>175</sup>

Cancerous and non-cancerous tissues from 12 patients undergoing surgery for colorectal cancer were analyzed using a handheld RS system. PCA and LDA resulted in 87.5% sensitivity, 82.6% specificity, and 85.1% accuracy for discrimination. Early cancer and advanced cancer tissue samples could also be differentiated with 85.7% sensitivity, 83.3% specificity, and 85.4% accuracy.<sup>176</sup> A final study performed using a handheld instrument involved analysis of tissue samples from 20 patients who underwent surgery for colorectal cancer. PCA with ROC curve analysis could identify colorectal cancer with 85.1% accuracy.<sup>177</sup> Validation was not reported in either study.

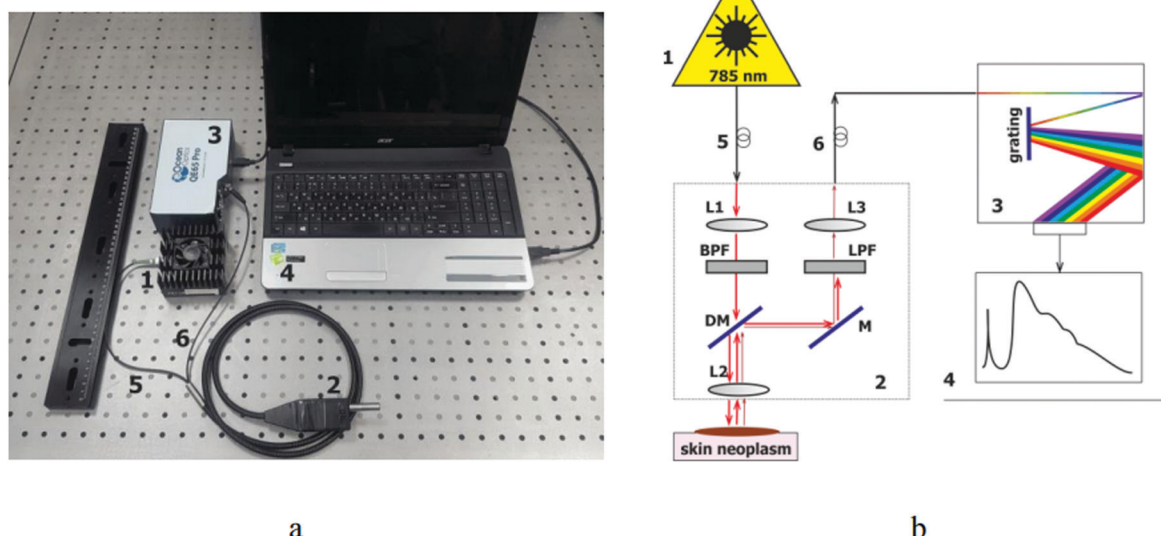


**Fig. 10** Details of the portable Raman system: (a) photo, (b) experimental scheme. (1 – laser module, 2 – optical Raman probe, 3 – spectrometer, 4 – PC, 5 – excitation fiber, 6 – collection fiber); 785 nm laser radiation is delivered to the optical detector by excitation fibers 5 (100  $\mu\text{m}$  diameter, 0.22 NA) and collimating lens L1, passes through the bandpass filter (BPF) to cut off unwanted fluorescence and Raman signal generated inside the optical fiber. The dichroic mirror (DM) transmit laser radiation to lens L2, which focuses exciting radiation onto the sample. The same lens L2 collects Raman, AF, and backscattered radiation. DM and mirror (M) transmit collected radiation on longpass filter (LPF) to cut off exciting laser radiation. The scattered radiation transmits to multichannel spectrograph by matching lens L3, and collection fibers 6 (200  $\mu\text{m}$  diameter, 0.22 NA) Reprinted with permission from Y. A. Khristoforova, I. A. Bratchenko, O. O. Myakinin, D. N. Artemyev, A. A. Moryatov, A. E. Orlov, S. V. Kozlov, V. P. Zakharov, Portable spectroscopic system for *in vivo* skin neoplasms diagnostics by Raman and autofluorescence analysis, *J. Biophotonics*, 2019, **12**, e201800400. Copyright (2019) John Wiley & Sons, Inc.

However, while only few diseases were recently explored using handheld RS instruments, the potential they hold is limitless and deserves further exploration in the future.

#### 4.5. Other variations of Raman spectroscopy

In addition to the aforementioned variations of RS, there remains several others which were used recently in only a very few number of studies. For example, coherent anti-Stokes Raman scattering (CARS) was used for the fast and non-invasive diagnosis of cervical cancer. CARS utilizes multiple photons to produce a coherent effect, thus producing a stronger anti-Stokes Raman signal. In addition to CARS, SHG/TPF imaging was performed on Pap smears from patients with specimens negative for intraepithelial lesions or malignancy and low-grade and high-grade squamous intraepithelial lesions. Deep CNNs were trained with CARS, SHG/TPR, and Raman imaging independently. Each method could most advantageously categorize the normal and cancerous Pap smears with 100% accuracy after LOSOCV.<sup>178</sup>

An alternative approach was used for studying colorectal cancer based on a high-throughput RS system. The high-throughput analysis of blood serum from 30 cancer patients and 30 healthy controls combined with PLS-DA gave a diagnostic sensitivity and specificity of 83% each after CV for classifying colorectal cancer.<sup>179</sup> These results are not necessarily an improvement on other studies but do importantly allow for many samples to be probed quickly, saving time and effort for generating diagnoses.

Finally, short wave infrared (SWIR) dispersive RS was used for differentiating normal and malignant renal samples. SWIR RS dramatically reduces background fluorescence in specific bulk tissue specimens. A sparse multinomial logistic regression with ROC curve analysis achieved 95.8% sensitivity and 88.8% specificity for diagnosis after LOSOCV, indicating the advantages of SWIR RS for detecting the renal malignancies.<sup>180</sup>

Many different variations of RS have been employed for reaching the same goal of successful medical diagnostic applications. While some systems perform better than others, it remains that the most successful results tend to be seen using spontaneous RS. This is an interesting observation, as it indicates that the more complicated and laborious Raman spectroscopic set-ups are not necessary for achieving better and more accurate screening and diagnostic results.

## 5. Critical evaluation

Many of the accomplishments made in the last two years represent minor, but important, victories for the field of medical diagnostics. Many of these research articles capitalize on basic chemometric methods to address complicated issues in small, proof-of-concept studies. Despite the lack of complexity, some of the most successful work was done using these basic methods. Importantly, these experiments are crucial for laying the groundwork from which researchers can build upon before spending costly time and resources to investigate larger *in vivo* applications of the method. Furthermore, as the method continues to develop, the variety of diseases which are examined continuously expand,

opening new doors for future research. Within the last two years alone, a vast amount of research has been conducted which capitalizes on the advantages of Raman spectroscopy and machine learning for screening and diagnosing a wide assortment of ailments and diseases. It is clear the method of RS itself is incredibly advantageous for being a diagnostic tool. It is specific, objective, inexpensive and easy to use, and can be sensitive and non-invasive. The aforementioned summarized articles aim to support the conclusion that Raman spectroscopy has extreme potential to be used in clinical settings for real-time accurate and definitive universal medical diagnostics.

However, it is important to acknowledge the pitfalls as well as the advantages of the herein described manuscripts and studies. Firstly, some of the studies which are summarized in this review use a very small sample pool; while this by itself is a nonissue, it remains to be seen that larger, statistically significant, trials are absolutely necessary to perform so that scientists can fully evaluate the method and its reliability. Those studies which do not provide quantitative results, and instead are qualitative in nature (*e.g.* utilize unsupervised machine learning methods), require further validation to ensure that objective results and diagnoses can be achieved, instead of subjective results based on clustering of data.

Along that line, not all studies reported validation of the machine learning methods. That is, data of samples from donors which were not used to build the statistical algorithms were not consistently used to then test the performance of the model. This validation, referred to as external validation, is absolutely crucial for establishing the trustworthiness of a statistical method. External validation functions to ensure there are no other factors which may be influencing differentiation. In fact, successful external validation is an indication that unlabeled spectra can accurately be predicted as belonging to a class based on the spectral changes that result from differences in disease state alone, thus indicating the method will not be affected by other biological factors. Successful external validation further indicates the developed method does not suffer from being over-fit to the data used to build it, and suggests the model is not biased and can be deemed both statistically and realistically ready for use in clinical settings. However, external validation cannot always be easily performed. Additional samples (from new donors) are required for this validation step; these additional samples may not be easily attainable due to problems with funding, donor participation, and/or lack of collaboration. These can prevent researchers from performing this crucial step, leading to potentially overestimating the capability of the method. This is an area of major concern which needs to be addressed in future progression of this work, as it is vital to apply unseen data to the prediction models to determine whether or not they perform adequately.

Lastly, the majority of the studies discussed herein are considered *ex vivo* experiments. To bring this work into clinical settings, additional progress toward *in vivo* research is absolutely crucial. The overarching goal is to apply the method directly into medical settings; it is thus necessary to continue advancing the research using fiber-optic probes and handheld

**Table 2** Summary of types of studies related to diagnosing cancer using RS and chemometrics since 2018

Type of cancer	# of studies	# of <i>in vivo</i> vs. <i>ex vivo</i>	Validation schemes used
Bladder	6	<i>Ex vivo</i> – 6	Cross validation – 6
Brain	8	<i>Ex vivo</i> – 6 <i>In situ</i> – 1 <i>In vivo</i> – 1	Cross validation – 4 NVR – 4
Breast	12	<i>Ex vivo</i> – 12	Cross validation – 9 External validation – 2 NVR – 1
Cervical	5	<i>Ex vivo</i> – 5	Cross validation – 4 External validation – 1
Colorectal	6	<i>Ex vivo</i> – 6	Cross validation – 2 NVR – 4
Esophageal	1	<i>Ex vivo</i> – 1	External validation – 1
Gastric	3	<i>Ex vivo</i> – 3	Cross validation – 2 NVR – 1
Head and neck	5	<i>Ex vivo</i> – 4 <i>In vivo</i> – 1	Cross validation – 4 NVR – 1
Leukemia	4	<i>Ex vivo</i> – 4	Cross validation – 3 NVR – 1
Liver	4	<i>Ex vivo</i> – 4	Cross validation – 2 External validation – 1 NVR – 1
Lung	11	<i>Ex vivo</i> – 10 <i>In vivo</i> – 1	Cross validation – 6 NVR – 5
Lymphatic	2	<i>Ex vivo</i> – 2	External validation – 1 NVR – 1
Oral	7	<i>Ex vivo</i> – 7	Cross validation – 6 External validation – 1
Ovarian	3	<i>Ex vivo</i> – 3	Cross validation – 2 NVR – 1
Pancreatic	2	<i>Ex vivo</i> – 2	External validation – 1 NVR – 1
Prostate	8	<i>Ex vivo</i> – 8	Cross validation – 4 External validation – 2 NVR – 2
Renal	1	<i>Ex vivo</i> – 1	Cross validation – 1
Skin	6	<i>Ex vivo</i> – 3 <i>In vivo</i> – 3	Cross validation – 4 External validation – 1 NVR – 1
Thyroid	4	<i>Ex vivo</i> – 4	Cross validation – 3 NVR – 1
Tongue	2	<i>Ex vivo</i> – 2	Cross validation – 1 NVR – 1
p53 biomarker	1	<i>Ex vivo</i> – 1	Cross validation – 1

NVR = no validation reported.

instruments which are better equipped for *in vivo* analysis but which have not been used to investigate all illnesses.

A summary of the types of diseases analyzed, the validation used, and whether the study was performed *in vivo* or *ex vivo* for cancer and all other diseases is seen in Tables 2 and 3, respectively.

While not all studies are perfect, there are many which demonstrate ideal scenarios. The epitome of a successful study would be one in which a statistically significant number of donors is analyzed, and optimal performance of the model is achieved during both cross-validation and external validation steps. Several studies reviewed here satisfy these requirements and are considered reliable, and the potential exists for further expansion on those studies which need it.

It is interesting to note the prediction performance results of studies which were accomplished using data from spontaneous

RS *versus* SERS or other variations of RS. In most cases, the performance results of the machine learning models are comparable; some studies performed using SERS or other forms of RS achieve better results than those performed using spontaneous RS, although only marginally. It can thus be hypothesized that spontaneous RS is sufficient for achieving just as successful results, and the complicated and sometimes time-consuming set ups and procedures involved in other variations of RS are not necessary for generating accurate diagnoses. However, it should still be noted that there are some situations where it is suggested spontaneous RS is not optimally suitable, including for conducting deep tissue analysis. In this scenario, spatially offset Raman spectroscopy (SORS) is a preferred method. While research has progressed significantly using SORS, a combination of the method with chemometrics has seldom been recently reported. For more information on spatially offset RS, the reader is referred to external work.<sup>181–183</sup> Further, CARS can be seen as a preferred alternative method due to the lack of fluorescence interference, allowing for measurements to be made more rapidly as compared to spontaneous RS. Unfortunately, this is another method which is rarely used by scientists due to its more complicated and time-consuming nature, as illustrated by only one publication which used CARS for medical diagnostics in the last few years.

With that being said, the application of devices such as fiber-optic probes and handheld instruments are areas which require further exploration. To one day bring the technology into clinical settings, smaller, portable RS instruments are required. Those studies reported in this review which utilize probes and handheld instruments, while successful, require their own further expansion and improvement. Interestingly, probes and portable instruments have already found themselves at the patients' bedside, as is evident from the aforementioned studies and as reviewed by others.<sup>184,185</sup> As these technologies continue to advance, additional research may be accomplished to support the introduction of these methods to clinical settings.

Two remaining challenges exist for establishing RS within medical settings for screening and diagnostic purposes. First is the need to standardize the instrument across all users, which includes developing regulations regarding factors such as laser power and excitation wavelength, which instruments to use, and the parameters needed to analyze the data. Additionally, a unification of machine learning analysis will be required. To make the method as simple as possible, it would be ideal to consolidate the techniques which are employed for making classification decisions. An automatic and user-friendly system will be the most useful for high throughput, rapid, and accurate diagnoses.

The second, and equally important, issue is the need to bridge the gap in trust between medical professionals and analytical chemists, and specifically, spectroscopists. It is vital for the medical community to understand the methodology and its dramatic advantages to begin to trust the process and allow for it to make life-altering diagnoses. This will only happen if increasingly more scientists continue to advance the field forward, spreading the word at conferences and

**Table 3** Summary of types of studies related to diagnosing all other diseases using RS and chemometrics since 2018

Disease category	# of studies	# of <i>in vivo</i> vs. <i>ex vivo</i>	Validation used
Bacterial infection	4	<i>Ex vivo</i> – 4	Cross validation – 3 NVR – 1
Parasitic infection	1	<i>Ex vivo</i> – 1	External validation – 1
Viral infection	8	<i>Ex vivo</i> – 8	Cross validation – 4 External validation – 2 NVR – 2
Blood disorder	2	<i>Ex vivo</i> – 2	Cross validation – 1 NVR – 1
Diabetes	4	<i>Ex vivo</i> – 3	Cross validation – 2 <i>In vivo</i> – 1
Kidney diseases & related	3	<i>Ex vivo</i> – 3	Cross validation – 1 External validation – 2
Heart diseases & related	2	<i>Ex vivo</i> – 2	Cross validation – 2
Thyroid diseases & related	3	<i>Ex vivo</i> – 3	External validation – 3
Autoimmune disease	3	<i>Ex vivo</i> – 3	Cross validation – 1 External validation – 2
Neurodegenerative disease	6	<i>Ex vivo</i> – 6	Cross validation – 3 External validation – 3
Ochronosis	1	<i>Ex vivo</i> – 1	NVR – 1
Ocular disease	1	<i>Ex vivo</i> – 1	External validation – 1
Osteoarthritis	1	<i>Ex vivo</i> – 1	Cross validation – 1
Endometriosis	1	<i>Ex vivo</i> – 1	External validation – 1
Prenatal disease	1	<i>Ex vivo</i> – 1	NVR – 1
Respiratory disease & related	3	<i>Ex vivo</i> – 3	Cross validation – 2 External validation – 1
Sexually transmitted disease	1	<i>In vitro</i> – 1	Cross validation – 1

NVR = no validation reported.

professional meetings, and encouraging collaborations with those in the medical community. It is expected that by sharing information, the medical community may learn more about this technique and be encouraged to practice it in their own settings. Further, large-scale multi-center trials between spectroscopists and medical communities will need to occur to demonstrate the feasibility of the method for full-time clinical introduction. If these prove successful, the pathway toward revolutionizing medical diagnostics becomes clear.

Both of these issues will require tremendous collaboration and willingness of experts in both fields to accomplish; ideally, the potential of the method and its ability to transform the field of medical diagnostics will be enough to encourage those brilliant minds to take on such a grueling, but rewarding, task. Several prominent researchers delve further into the considerations required for translating RS into clinical settings.<sup>8,18,21,29,186</sup> Although there is much work to be done, it remains that Raman spectroscopy in combination with machine learning methods has shown incredible potential to be used as a novel universal screening and disease detection method which is non-invasive, objective, accurate and definitive.

## 6. Conclusions

Receiving a medical diagnosis for a condition an individual has should be a simple, definitive, and straightforward process. Unfortunately, for many people around the world, a diagnosis is either impossible to make due to insufficient diagnostic tests

or resources, unreliability of the diagnostic test, or inability to generate a diagnosis until a disease has progressed too far. Raman spectroscopy in combination with machine learning techniques is proposed here as a universal method for medical diagnostics which is fast, accurate, objective, and definitive. The method itself is inherently non-invasive, easy-to-use, and has the potential to easily be implemented into clinical settings. This review highlights the momentous research which has been conducted since 2018 by researchers around the world who have utilized Raman spectroscopy for screening for and diagnosing a wide range of ailments and diseases. Although there remains work for improvement and hurdles to overcome before bringing the method into clinical settings, there is a great and promising potential for Raman spectroscopy in combination with chemometrics to become the first universal method for medical diagnostics.

## List of key abbreviations

RS	Raman spectroscopy
PCA	Principal component analysis
SVM	Support vector machine
LOOCV	Leave-one-out cross-validation
KNN	K-Nearest neighbor
CV	Cross-validation
PLS-DA	Partial least squares discriminant analysis
PC-LDA	Principal component linear discriminant analysis
LOSOCV	Leave-one-sample-out cross-validation
ROC	Receiver operating characteristic
AUC	Area under the curve
QDA	Quadratic discriminant analysis
MCR	Multivariate curve resolution
ALS	Alternative least squares
OPLS	Orthogonal partial least squares
FDA	Factorial discriminant analysis
ANN	Artificial neural networks
GA	Genetic algorithm
RF	Random forest
SERS	Surface enhanced Raman spectroscopy
DUVRS	Deep-ultraviolet Raman spectroscopy
LTRS	Laser tweezer Raman spectroscopy
SERDS	Shifted excitation Raman difference spectroscopy
CNN	Convolutional neural networks
CARS	Coherent anti-Stokes Raman spectroscopy

## Conflicts of interest

There are no conflicts to declare.

## Acknowledgements

N. M. R. was supported by NIH training grant T32 GM13206.

## References

- 1 F. Lussier, V. Thibault, B. Charron, G. Q. Wallace and J.-F. Masson, *TrAC, Trends Anal. Chem.*, 2020, **124**, 115796.
- 2 M. A. Fikiet, S. R. Kandasammy, E. Mistek, Y. Ahmed, L. Halámková, J. Bueno and I. K. Lednev, *Spectrochim. Acta, Part A*, 2018, **197**, 255–260.
- 3 S. J. Mazivila and A. C. Olivier, *TrAC, Trends Anal. Chem.*, 2018, **108**, 74–87.
- 4 D. DePaoli, É. Lemoine, K. Ember, M. Parent, M. Prud'homme, L. Cantin, K. Petrecca, F. Leblond and D. C. Côté, *J. Biomed. Opt.*, 2020, **25**, 050901.
- 5 M. Binkhonain and L. Zhao, *Expert Systems with Applications: X*, 2019, **1**, 100001.
- 6 T. P. Carvalho, F. A. A. M. N. Soares, R. Vita, R. D. P. Francisco, J. P. Basto and S. G. S. Alcalá, *Comput. Ind. Eng.*, 2019, **137**, 106024.
- 7 F. Zantalis, G. Koulouras, S. Karabetsos and D. Kandris, *Future Internet*, 2019, **11**, 94.
- 8 M. J. Baker, H. J. Byrne, J. Chalmers, P. Gardner, R. Goodacre, A. Henderson, S. G. Kazarian, F. L. Martin, J. Moger, N. Stone and J. Sulé-Suso, *Analyst*, 2018, **143**, 1735–1757.
- 9 M. J. Baker, S. R. Hussain, L. Lovergne, V. Untereiner, C. Hughes, R. A. Lukaszewski, G. Thiéfin and G. D. Sockalingum, *Chem. Soc. Rev.*, 2016, **45**, 1803–1818.
- 10 L. B. Leal, M. S. Nogueira, R. A. Canevari and L. F. C. S. Carvalho, *Photodiagn. Photodyn. Ther.*, 2018, **24**, 237–244.
- 11 S. Pahlow, K. Weber, J. Popp, R. W. Bayden, K. Kochan, A. Rüther, D. Perez-Guaita, P. Heraud, N. Stone, A. Dudgeon, B. Gardner, R. Reddy, D. Mayerich and R. Bhargava, *Appl. Spectrosc.*, 2018, **72**, 52–84.
- 12 A.-I. Henry, B. Sharma, M. F. Cardinal, D. Kurouski and R. P. Van Duyne, *Anal. Chem.*, 2016, **88**, 6638–6647.
- 13 S. McAughtrie, K. Faulds and D. Graham, *J. Photochem. Photobiol., C*, 2014, **21**, 40–53.
- 14 S. Laing, L. E. Jamieson, K. Faulds and D. Graham, *Nat. Rev. Chem.*, 2017, **1**, 0060.
- 15 T. J. Moore, A. S. Moody, T. D. Payne, G. M. Sarabia, A. R. Daniel and B. Sharma, *Biosensors*, 2018, **8**, 46.
- 16 J.-F. Masson and K. S. McKeating, in *Advances in Electrochemical Science and Engineering: Nanopatterned and Nanoparticle-Modified Electrodes*, ed. R. C. Alkire, P. N. Bartlett and J. Lipkowski, John Wiley & Sons, 2017, vol. 17.
- 17 E. Cordero, I. Latka, C. Matthäus, I. W. Schie and J. Popp, *J. Biomed. Opt.*, 2018, **23**, 071210.
- 18 M. Jermyn, J. Desroches, K. Aubertin, K. St-Arnaud, W.-J. Madore, E. De Montigny, M.-C. Guiot, D. Trudel, B. C. Wilson, K. Petrecca and F. Leblond, *Phys. Med. Biol.*, 2016, **61**, R370.
- 19 G. W. Auner, S. K. Koya, C. Huang, B. Broadbent, M. Trexler, Z. Auner, A. Elias, K. C. Mehne and M. A. Brusatori, *Cancer Metastasis Rev.*, 2018, **37**, 691–717.
- 20 N. M. Ralbovsky and I. K. Lednev, *Spectrochim. Acta, Part A*, 2019, **219**, 463–487.
- 21 I. P. Santos, E. M. Barroso, T. C. Bakker Schut, P. J. Caspers, C. G. F. van Lanschot, D.-H. Choi, M. F. van der Kamp, R. W. H. Smits, R. van Doorn, R. M. Verdijk, V. Noordhoek Hejt, J. H. von der Thüsen, C. H. M. van Deurzen, L. B. Koppert, G. J. L. H. van Leenders, P. C. Ewing-Graham, H. C. van Doorn, C. M. F. Dirven, M. B. Bussstra, J. Hardillo, A. Sewnaik, I. ten Hove, H. Mast, D. A. Monserez, C. Meeuwis, T. Nijsten, E. B. Wolvius, R. J. Baatenburg de Jong, G. J. Puppels and S. Koljenović, *Analyst*, 2017, **142**, 3025–3047.
- 22 E. Upchurch, M. Isabelle, G. R. Lloyd, C. Kendall and H. Barr, *Expert Rev. Mol. Diagn.*, 2018, **18**, 245–258.
- 23 K. J. I. Ember, M. A. Hoeve, S. L. McAughtrie, M. S. Bergholt, B. J. Dwyer, M. M. Stevens, K. Faulds, S. J. Forbes and C. J. Campbell, *npj Regener. Med.*, 2017, **2**, 12.
- 24 C. Krafft and J. Popp, *Transl. Biophotonics*, 2019, **1**, e201900018.
- 25 C. Krafft and J. Popp, *Anal. Bioanal. Chem.*, 2015, **407**, 699–717.
- 26 K. Eberhardt, C. Stiebing, C. Matthäus, M. Schmitt and J. Popp, *Expert Rev. Mol. Diagn.*, 2015, **15**, 773–787.
- 27 K. Kong, C. Kendall, N. Stone and I. Notinger, *Adv. Drug Delivery Rev.*, 2015, **89**, 121–134.
- 28 A. L. Mitchell, K. B. Gajjar, G. Theophilou, F. L. Martin and P. L. Martin-Hirsch, *J. Biophotonics*, 2014, **7**, 153–165.
- 29 I. Pence and A. Mahadevan-Jansen, *Chem. Soc. Rev.*, 2016, **45**, 1958–1979.
- 30 K. Hernández-Vidales, E. Guevara, V. Olivares-Illana and F. J. González, *J. Raman Spectrosc.*, 2019, **50**, 1388–1394.
- 31 D. Bovenkamp, R. Sentosa, E. Rank, M. T. Erkkilä, F. Placzek, J. Püls, W. Drexler, R. A. Leitgeb, N. Garstka, S. F. Shariat, C. Stiebing, I. W. Schie, J. Popp, M. Andreana and A. Unterhuber, *Appl. Sci.*, 2018, **8**, 2371.
- 32 H. Abramczyk and A. Imiela, *Spectrochim. Acta, Part A*, 2018, **188**, 8–19.
- 33 K. Mehta, A. Atak, A. Sahu, S. Srivastava and C. M. Krishna, *Analyst*, 2018, **143**, 1916–1923.
- 34 D. Bury, G. Faust, M. Paraskevaidi, K. M. Ashton, T. P. Dawson and F. L. Martin, *Anal. Lett.*, 2018, **52**, 575–587.
- 35 J. Depciuch, B. Tołpa, P. Witek, K. Szmuc, E. Kaznowska, M. Osuchowski, P. Król and J. Cebulski, *Spectrochim. Acta, Part A*, 2020, **225**, 117526.
- 36 Y. Zhou, C.-H. Liu, Y. Pu, B. Wu, T. A. Nguyen, G. Cheng, L. Zhou, K. Zhu, J. Chen, Q. Li and R. R. Alfano, *J. Innov. Opt. Health Sci.*, 2019, **12**, 1950010.
- 37 O. Fallahzadeh, Z. Dehghani-Bidgoli and M. Assarian, *Lasers Med. Sci.*, 2018, **33**, 1799–1806.
- 38 M. Marro, C. Nieva, A. de Juan and A. Sierra, *Anal. Chem.*, 2018, **90**, 5594–5602.
- 39 F. M. Lyng, D. Traynor, T. N. Q. Nguyen, A. D. Meade, F. Rakib, R. Al-Saady, E. Goormaghtigh, K. Al-Saad and M. H. Ali, *PLoS One*, 2019, **14**, e0212376.
- 40 V. Dubey, A. Ahmad, A. Butola, D. Qaiser, A. Srivastava and D. S. Mehta, *Appl. Opt.*, 2019, **58**, A112–A119.
- 41 A. C. S. Talari, S. Rehman and I. U. Rehman, *Expert Rev. Mol. Diagn.*, 2019, **19**, 929–940.

- 42 M. Albayrak, O. Senol, F. Demirkaya-Miloglu, M. Calik and Y. Kadioglu, *Bratisl. Lek. Listy*, 2019, **120**, 184–187.
- 43 K. Chithra, P. Aruna, S. Vijayaraghavan, S. G. Prasad and S. Ganesan, *Vib. Spectrosc.*, 2019, **105**, 102982.
- 44 H. F. Nargis, H. Nawaz, A. Ditta, T. Mahmood, M. I. Majeed, N. Rashid, M. Muddassar, H. N. Bhatti, M. Saleem, K. Jilani, F. Bonnier and H. J. Byrne, *Spectrochim. Acta, Part A*, 2019, **222**, 117210.
- 45 A. Daniel, A. Prakasaraao and S. Ganesan, *Spectrochim. Acta, Part A*, 2018, **190**, 409–416.
- 46 S. Duraipandian, D. Traynor, P. Kearney, C. Martin, J. J. O’Leary and F. M. Lyng, *Sci. Rep.*, 2018, **8**, 15048.
- 47 C. Zheng, S. Qing, J. Wang, G. Lü, H. Li, X. Lü, C. Ma, J. Tang and X. Yue, *Photodiagn. Photodyn. Ther.*, 2019, **27**, 156–161.
- 48 P. Raja, P. Aruna, D. Koteeswaran and S. Ganesan, *Vib. Spectrosc.*, 2019, **102**, 1–7.
- 49 J. Gala de Pablo, F. J. Armistead, S. A. Peyman, D. Bonthron, M. Lones, S. Smith and S. D. Evans, *J. Raman Spectrosc.*, 2018, **49**, 1323–1332.
- 50 I. Maitra, C. L. M. Morais, K. M. G. Lima, K. M. Ashton, R. S. Date and F. L. Martin, *J. Biophotonics*, 2020, **13**, e201960132.
- 51 M. Bahreini, A. Hosseinzadegan, A. Rashidi, S. R. Miri, H. R. Mirzaei and P. Hajian, *Talanta*, 2019, **204**, 826–832.
- 52 S. Khan, R. Ullah, S. Shahzad, S. Javaid and A. Khan, *Optik*, 2018, **157**, 565–570.
- 53 O. Senol and M. Albayrak, *Curr. Opt. Photonics*, 2019, **3**, 150–153.
- 54 M. A. Mascarella, A. Alrasheed, N. Fnais, O. Gourgas, G. Jalani, M. Cerruti and M. A. Tewfik, *Otolaryngol.–Head Neck Surg.*, 2018, **159**, 587–589.
- 55 S. Managò, P. Mirabelli, M. Napolitano, G. Zito and A. C. De Luca, *J. Biophotonics*, 2018, **11**, e201700265.
- 56 J. L. González-Solís, *PLoS One*, 2019, **14**, e0213621.
- 57 A. M. da Silva, F. S. A. de Siqueira e Oliveira, P. L. de Brito and L. Silveira Jr, *J. Biomed. Opt.*, 2018, **23**, 107002.
- 58 H. Wang, S. Zhang, L. Wan, H. Sun, J. Tan and Q. Su, *Spectrochim. Acta, Part A*, 2018, **201**, 34–38.
- 59 A. Sinica, K. Brožáková, T. Brůha and J. Votruba, *Spectrochim. Acta, Part A*, 2019, **219**, 257–266.
- 60 Q. Zheng, J. Li, L. Yang, B. Zheng, J. Wang, N. Lv, J. Luo, F. L. Martin, D. Liu and J. He, *Analyst*, 2020, **145**, 385–392.
- 61 B. Shiramizu, R. Oda, N. Kamada, M. A. Garcia, T. Shieh, T. A. Maeda, S. Y. Choi, E. Lim and A. Misra, *J. Biol. Med. Sci.*, 2018, **2**, 105.
- 62 J. V. Rau, F. Marini, M. Fosca, C. Cippitelli, M. Rocchia and A. Di Napoli, *Talanta*, 2019, **194**, 763–770.
- 63 F. L. J. Cals, T. C. B. Schut, P. J. Caspers, R. J. Baatenburg de Jong, S. Koljenović and G. J. Puppels, *Analyst*, 2018, **143**, 4090–4102.
- 64 A. Sahu, P. Gera, A. Malik, S. Nair, P. Chaturvedi and C. M. Krishna, *J. Biophotonics*, 2019, **12**, e201800334.
- 65 A. Ghosh, S. Raha, S. Dey, K. Chatterjee, A. R. Chowdhury and A. Barui, *Analyst*, 2019, **144**, 1309–1325.
- 66 M.-J. Jeng, M. Sharma, L. Sharma, T.-Y. Chao, S.-F. Huang, L.-B. Chang, S.-L. Wu and L. Chow, *J. Clin. Med.*, 2019, **8**, 1313.
- 67 A. Hole, G. Tyagi, A. Sahu, R. Shaikh and C. M. Krishna, *Vib. Spectrosc.*, 2018, **98**, 35–40.
- 68 F. L. Magalhães, A. M. C. Machado, E. Paulino, S. K. Sahoo, A. M. de Paula, A. M. Garcia, I. Barman, J. S. Soares and M. Mamede, *J. Biomed. Opt.*, 2018, **23**, 121613.
- 69 X. Feng, M. C. Fox, J. S. Reichenberg, F. C. P. S. Lopes, K. R. Sebastian, M. K. Markey and J. W. Tunnell, *Biomed. Opt. Express*, 2019, **10**, 104–118.
- 70 I. P. Santos, R. van Doorn, P. J. Caspers, T. C. B. Schut, E. M. Barroso, T. E. C. Nijsten, V. N. Hegt, S. Koljenović and G. J. Puppels, *Br. J. Cancer*, 2018, **119**, 1339–1346.
- 71 A. M. Ferreira Lima, C. R. Daniel, R. S. Navarro, B. Bodanese, C. A. Pasqualucci, M. T. T. Pacheco, R. A. Zângaro and L. Silveira Jr, *Vib. Spectrosc.*, 2019, **100**, 131–141.
- 72 J. Depciuch, A. Stanek-Widera, D. Skrzypiec, D. Lange, M. Biskup-Frużyńska, K. Kiper, J. Stanek-Tarkowska, M. Kula and J. Cebulski, *J. Pharm. Biomed. Anal.*, 2019, **170**, 321–326.
- 73 O. Senol, M. Albayrak, F. Demirkaya Miloglu, Y. Kadioglu and M. Calik, *Anal. Lett.*, 2018, **51**, 229–235.
- 74 D. O’Dea, M. Bongiovanni, G. P. Sykiotis, P. G. Ziros, A. D. Meade, F. M. Lyng and A. Malkin, *Cytopathology*, 2019, **30**, 51–60.
- 75 M. A. S. De Oliveira, M. Campbell, A. M. Afify, E. C. Huang and J. W. Chan, *Biomed. Opt. Express*, 2019, **10**, 4411–4421.
- 76 S. Khan, R. Ullah, S. Shahzad, N. Anbreem, M. Bilal and A. Khan, *Photodiagn. Photodyn. Ther.*, 2018, **24**, 286–291.
- 77 S. K. Koya, M. Brusatori, J. V. Martin, S. Urgelevic, C. Huang, D. M. Liberati, G. W. Auner and L. N. Diebel, *J. Surg. Res.*, 2018, **232**, 195–201.
- 78 A. Ditta, H. Nawaz, T. Mahmood, M. I. Majeed, M. Tahir, N. Rashid, M. Muddassar, A. A. Al-Saadi and H. J. Byrne, *Spectrochim. Acta, Part A*, 2019, **221**, 117173.
- 79 A. Sohail, S. Khan, R. Ullah, S. A. Qureshi, M. Bilal and A. Khan, *Biomed. Opt. Express*, 2018, **9**, 2041–2055.
- 80 D. Tong, C. Chen, J. Zhang, G. Lv, X. Zheng, Z. Zhang and X. Lv, *Photodiagn. Photodyn. Ther.*, 2019, **28**, 248–252.
- 81 S. Khan, R. Ullah, A. Khan, R. Ashraf, H. Ali, M. Bilal and M. Saleem, *Photodiagn. Photodyn. Ther.*, 2018, **23**, 89–93.
- 82 T. Mahmood, H. Nawaz, A. Ditta, M. I. Majeed, M. A. Hanif, N. Rashid, H. N. Bhatti, H. F. Nargis, M. Saleem, F. Bonnier and H. J. Byrne, *Spectrochim. Acta, Part A*, 2018, **200**, 136–142.
- 83 S. K. Patel, N. Rajora, S. Kumar, A. Sahu, S. K. Kochhar, C. M. Krishna and S. Srivastava, *Anal. Chem.*, 2019, **91**, 7054–7062.
- 84 K. Naseer, A. Amin, M. Saleem and J. Qazi, *Spectrochim. Acta, Part A*, 2019, **206**, 197–201.
- 85 L. F. D. C. E. S. de Carvalho and M. S. Nogueira, *Photodiagn. Photodyn. Ther.*, 2020, **30**, 101765.
- 86 L. Jacobi, V. H. Damle, B. Rajeswaran and Y. R. Tischler, *R. Soc. Open Sci.*, 2020, DOI: 10.17605/OSF.IO/Y54H3.
- 87 Y.-T. Yeh, K. Gulino, Y. Zhang, A. Sabestien, T.-W. Chou, B. Zhou, Z. Lin, I. Albert, H. Lu, V. Swaminathan, E. Ghedin and M. Terrones, *Proc. Natl. Acad. Sci. U. S. A.*, 2020, **117**, 895–901.

- 88 W. R. da Silva, L. Silveira Jr and A. B. Fernandes, *Lasers Med. Sci.*, 2020, **35**, 1065–1074.
- 89 J. L. González-Solís, J. R. Villafan-Bernal, B. E. Martínez-Zéregua and S. Sánchez-Enríquez, *Lasers Med. Sci.*, 2018, **33**, 1791–1797.
- 90 C. Chen, L. Yang, J. Zhao, Y. Yuan, C. Chen, J. Tang, H. Yang, Z. Yan, H. Wang and X. Lv, *Optik*, 2020, **203**, 164043.
- 91 X. Cui, Z. Zhao, G. Zhang, S. Chen, Y. Zhao and J. Lu, *Biomed. Opt. Express*, 2018, **9**, 4175–4183.
- 92 X. Zheng, G. Lv, Y. Zhang, X. Lv, Z. Gao, J. Tang and J. Mo, *Spectrochim. Acta, Part A*, 2019, **215**, 244–248.
- 93 X. Zheng, G. Lv, G. Du, Z. Zhai, J. Mo and X. Lv, *IEEE Photonics J.*, 2018, **10**, 1–12.
- 94 Y. Du, G. Lü, G. Du, X. Lü, J. Tang, J. Liu, X. Yue, J. Mo and T. Sun, *Laser Phys. Lett.*, 2019, **16**, 065602.
- 95 A. Palermo, M. Fosca, G. Tabacco, F. Marini, V. Graziani, M. C. Santarsia, F. Longo, A. Lauria, R. Cesareo, I. Giovannoni, C. Taffon, M. Rocchia, S. Manfrini, P. Crucitti, P. Pozzilli, A. Crescenzi and J. V. Rau, *Anal. Chem.*, 2018, **90**, 847–854.
- 96 S. Fornasaro, A. Vicario, L. De Leo, A. Bonifacio, T. Not and V. Serigo, *Integr. Biol.*, 2018, **10**, 356–363.
- 97 N. M. Ralbovsky and I. K. Lednev, *Talanta*, 2021, **221**, 121642.
- 98 N. M. Ralbovsky, L. Halámková, K. Wall, C. Anderson-Hanley and I. K. Lednev, *J. Alzheimer's Dis.*, 2019, **71**, 1351–1359.
- 99 N. M. Ralbovsky and I. K. Lednev, *Biophotonics*, 2019, **4**, 33–37.
- 100 E. Ryzhikova, O. Kazakov, L. Halamkova, D. Celmins, P. Malone, E. Molho, E. A. Zimmerman and I. K. Lednev, *J. Biophotonics*, 2015, **8**, 584–596.
- 101 M. Paraskevaidi, C. L. M. Morais, D. E. Halliwell, D. M. A. Mann, D. Allsop, P. L. Martin-Hirsch and F. L. Martin, *ACS Chem. Neurosci.*, 2018, **9**, 2786–2794.
- 102 U. Parlatan, M. T. Inanc, B. Y. Ozgor, E. Oral, E. Bastu, M. B. Unlu and G. Basar, *Sci. Rep.*, 2019, **9**, 19795.
- 103 R. Ullah, S. Khan, F. Farman, M. Bilal, C. Krafft and S. Shahzad, *Biomed. Opt. Express*, 2019, **10**, 600–609.
- 104 A. M. Taylor, D. D. Jenks, V. D. Kammath, B. P. Norman, J. P. Dillon, J. A. Gallagher, L. R. Ranganath and J. G. Kerns, *Osteoarthr. Cartil.*, 2019, **27**, 1244–1251.
- 105 T. Sun, X. Xie, H. Li, G. Lv, X. Lv, J. Tang, X. Yue and J. Mo, *Laser Phys.*, 2019, **30**, 015701.
- 106 P. A. Mosier-Boss, *Nanomaterials*, 2017, **7**, 142.
- 107 D. Jin, X. Wang, B. Fu, T. Li, N. Chen, Z. Chen, H. Chen and S. Liu, *Int. J. Clin. Exp. Med.*, 2019, **12**, 5447–5453.
- 108 S. Chen, S. Zhu, X. Cui, W. Xu, C. Kong, Z. Zhang and W. Qian, *Biomed. Opt. Express*, 2019, **10**, 3533–3544.
- 109 Y. Zhang, X. Lai, Q. Zeng, L. Li, L. Lin, S. Li, Z. Liu, C. Su, M. Qi and Z. Guo, *Laser Phys.*, 2018, **28**, 035603.
- 110 V. Moisoiu, A. Socaciu, A. Stefancu, S. D. Iancu, I. Boros, C. D. Alecsa, C. Rachieriu, A. R. Chiorean, D. Eniu, N. Leopold, C. Socaciu and D. T. Eniu, *Appl. Sci.*, 2019, **9**, 806.
- 111 V. Moisoiu, A. Stefancu, D. Gulei, R. Boitor, L. Magdo, L. Raduly, S. Pasca, P. Kubelac, N. Mehterov, V. Chiş, M. Simon, M. Muresan, A. I. Irimie, M. Baciu, R. Stiufluc, I. E. Pavel, P. Achimas-Cadariu, C. Ionescu, V. Lazar, V. Sarafian, I. Notinger, N. Leopold and I. Berindan-Neagoe, *Int. J. Nanomed.*, 2019, **14**, 6165–6178.
- 112 Z. O. Králová, A. Oriňák, R. Oriňáková, O. Petruš, J. Macko, J. Radoňák, L. S. Lakyová, Z. Jurašeková, R. M. Smith, M. Strečková and K. Koval, *J. Biomed. Opt.*, 2018, **23**, 075002.
- 113 L. Guo, Y. Li, F. Huang, J. Dong, F. Li, X. Yang, S. Zhu and M. Yang, *J. Innovative Opt. Health Sci.*, 2019, **12**, 1950003.
- 114 X. Lin, L. Wang, H. Lin, D. Lin, J. Lin, X. Liu, S. Qiu, Y. Xu, G. Chen and S. Feng, *J. Biophotonics*, 2019, **12**, e201800327.
- 115 Q. Wu, S. Qiu, Y. Yu, W. Chen, H. Lin, D. Lin, S. Feng and R. Chen, *Biomed. Opt. Express*, 2018, **9**, 3413–3423.
- 116 M. Hassoun, J. Rüger, T. Kirchberger-Tolstik, I. W. Schie, T. Henkel, K. Weber, D. Cialla-May, C. Krafft and J. Popp, *Anal. Bioanal. Chem.*, 2018, **410**, 999–1006.
- 117 K. Lin, J. Xu, L. Li, F. Liao, X. Dong and J. Lin, *Laser Phys. Lett.*, 2018, **15**, 125601.
- 118 Y. Yu, Y. Lin, C. Xu, K. Lin, Q. Ye, X. Wang, S. Xie, R. Chen and J. Lin, *Biomed. Opt. Express*, 2018, **9**, 6053–6066.
- 119 L. Shao, A. Zhang, Z. Rong, C. Wang, X. Jia, K. Zhang, R. Xiao and S. Wang, *Nanomedicine*, 2018, **14**, 451–459.
- 120 K. Zhang, C. Hao, B. Man, C. Zhang, C. Yang, M. Liu, Q. Peng and C. Chen, *Vib. Spectrosc.*, 2018, **98**, 82–87.
- 121 K. Qian, Y. Wang, L. Hua, A. Chen and Y. Zhang, *Thorac. Cancer*, 2018, **9**, 1556–1561.
- 122 K. Zhang, X. Liu, B. Man, C. Yang, C. Zhang, M. Liu, Y. Zhang, L. Liu and C. Chen, *Biomed. Opt. Express*, 2018, **9**, 4345–4358.
- 123 K. Zhang, C. Hao, Y. Huo, B. Man, C. Zhang, C. Yang, M. Liu and C. Chen, *Lasers Med. Sci.*, 2019, **34**, 1849–1855.
- 124 X. Cao, Z. Wang, L. Bi and J. Zheng, *J. Chem.*, 2018, **2018**, 9012645.
- 125 H. Shin, H. Jeong, J. Park, S. Hong and Y. Choi, *ACS Sens.*, 2018, **3**, 2637–2643.
- 126 K. Liu, S. Jin, Z. Song, L. Jiang, L. Ma and Z. Zhang, *Vib. Spectrosc.*, 2019, **100**, 177–184.
- 127 K. Liu, S. Jin, Z. Song and L. Jiang, *Spectrochim. Acta, Part A*, 2020, **226**, 117632.
- 128 L. Xue, B. Yan, Y. Li, Y. Tan, X. Luo and M. Wang, *Int. J. Nanomed.*, 2018, **13**, 4977–4986.
- 129 G. Chundayil Madathil, S. Iyer, K. Thankappan, G. S. Gowd, S. Nair and M. Koyakutty, *Adv. Healthcare Mater.*, 2019, **8**, 1801557.
- 130 J. Perumal, A. P. Mahyuddin, G. Balasundaram, D. Goh, C. Y. Fu, A. Kazakeviciute, U. Dinish, M. Choolani and M. Olivo, *Cancer Manage. Res.*, 2019, **11**, 1115–1124.
- 131 J. d. J. Zermeño-Nava, M. U. Martínez-Martínez, A. L. Rámirez-de-Ávila, A. C. Hernández-Arteaga, M. G. García-Valdivieso, A. Hernández-Cedillo, M. José-Yacamán and H. R. Navarro-Contreras, *J. Ovarian Res.*, 2018, **11**, 61.
- 132 M. Paraskevaidi, K. M. Ashton, H. F. Stringfellow, N. J. Wood, P. J. Keating, A. W. Rowbottom, P. L. Martin-Hirsch and F. L. Martin, *Talanta*, 2018, **189**, 281–288.

- 133 T.-D. Li, R. Zhang, H. Chen, Z.-P. Huang, X. Ye, H. Wang, A.-M. Deng and J.-L. Kong, *Chem. Sci.*, 2018, **9**, 5372–5382.
- 134 J. Carmicheal, C. Hayashi, X. Huang, L. Liu, Y. Lu, A. Krasnoslobodtsev, A. Lushnikov, P. G. Kshirsagar, A. Patel, M. Jain, Y. L. Lyubchenko, Y. Lu, S. K. Batra and S. Kaur, *Nanomedicine*, 2019, **16**, 88–96.
- 135 K. M. Koo, J. Wang, R. E. S. Richards, A. Farrell, J. W. Yaxley, H. Samaratunga, P. E. Teloken, M. J. Roberts, G. D. Coughlin, M. F. Lavin, P. N. Mainwaring, Y. Wang, R. A. Gardiner and M. Trau, *ACS Nano*, 2018, **12**, 8362–8371.
- 136 A. Stefancu, V. Moisoiu, R. Couti, I. Andras, R. Rahota, D. Crisan, I. E. Pavel, C. Socaciu, N. Leopold and N. Crisan, *Nanomedicine*, 2018, **13**, 2455–2467.
- 137 J. Pan, X. Shao, Y. Zhu, B. Dong, Y. Wang, X. Kang, N. Chen, Z. Chen, S. Liu and W. Xue, *Int. J. Nanomed.*, 2019, **14**, 431–440.
- 138 X. Chen, M. Tang, Y. Liu, J. Huang, Z. Liu, H. Tian, Y. Zheng, M. L. de la Chapelle, Y. Zhang and W. Fu, *Microchim. Acta*, 2019, **186**, 102.
- 139 A. Pérez, Y. A. Prada, R. Cabanzo, C. I. González and E. Mejía-Ospino, *Sens. Biosensing Res.*, 2018, **21**, 40–45.
- 140 A. Hernández-Cedillo, M. G. García-Valdivieso, A. C. Hernández-Arteaga, N. Patiño-Marín, Á. A. Vértiz-Hernández, M. José-Yacamán and H. R. Navarro-Contreras, *Oral Dis.*, 2019, **25**, 1627–1633.
- 141 D. Sebba, A. G. Lastovich, M. Kuroda, E. Fallows, J. Johnson, A. Ahoudi, A. N. Honko, H. Fu, R. Nielson, E. Carruthers, C. Diédiou, D. Ahmadou, B. Soropogui, J. Ruedas, K. Peters, M. Bartkowiak, N. F. Magassouba, S. Mboup, Y. B. Amor, J. H. Connor and K. Weidemaier, *Sci. Transl. Med.*, 2018, **10**, eaat0944.
- 142 J. Guo, Z. Rong, Y. Li, S. Wang, W. Zhang and R. Xiao, *Laser Phys.*, 2018, **28**, 075603.
- 143 H. Yang, C. Zhao, R. Li, C. Shen, X. Cai, L. Sun, C. Luo and Y. Yin, *Analyst*, 2018, **143**, 2235–2242.
- 144 A. Stefancu, M. Badarinza, V. Moisoiu, S. D. Iancu, O. Serban, N. Leopold and D. Fodor, *Anal. Bioanal. Chem.*, 2019, **411**, 5877–5883.
- 145 Q.-J. Zhang, Y. Chen, X.-H. Zou, W. Hu, X.-L. Lin, S.-Y. Feng, F. Chen, L.-Q. Xu, W.-J. Chen and N. Wang, *J. Biophotonics*, 2019, **12**, e201900012.
- 146 C. Carlomagno, M. Cabinio, S. Picciolini, A. Gualerzi, F. Baglio and M. Bedoni, *J. Biophotonics*, 2019, e201960033.
- 147 E. Ryzhikova, N. M. Ralbovsky, L. Halámková, D. Celmins, P. Malone, E. Molho, J. Quinn, E. A. Zimmerman and I. K. Lednev, *Appl. Sci.*, 2019, **9**, 3256.
- 148 W. Kim, S. H. Lee, J. H. Kim, Y. J. Ahn, Y.-H. Kim, J. S. Yu and S. Choi, *ACS Nano*, 2018, **12**, 7100–7108.
- 149 C. D. Bocsa, V. Moisoiu, A. Stefancu, L. F. Leopold, N. Leopold and D. Fodor, *Nanomedicine*, 2019, **20**, 102012.
- 150 B. N. Zamora-Mendoza, R. Espinosa-Tanguma, M. G. Ramirez-Elias, R. Cabrera-Alonso, G. Montero-Moran, D. Portales-Perez, J. A. Rosales-Romo, J. F. Gonzalez and C. Gonzalez, *Photodiagn. Photodyn. Ther.*, 2019, **27**, 85–91.
- 151 J. Lin, X. Lin, C. Hu, P. Bai, H. Yang, Y. Dai, H. Qiu, M. Lin, S. Feng and J. Pan, *Laser Phys. Lett.*, 2018, **15**, 095703.
- 152 Y. Chen, W. R. Premasiri and L. D. Ziegler, *Sci. Rep.*, 2018, **8**, 5163.
- 153 O. Žukovskaja, S. Kloß, M. G. Blango, O. Ryabchikov, O. Kniemeyer, A. A. Brakhage, T. W. Bocklitz, D. Cialla-May, K. Weber and J. R. Popp, *Anal. Chem.*, 2018, **90**, 8912–8918.
- 154 N. M. Ralbovsky, V. Egorov, E. Moskovets, P. Dey, B. K. Dey and I. K. Lednev, *Cancer Stud. Mol. Med.*, 2019, **5**, 1–10.
- 155 M. Liu, X. Liu, Z. Huang, X. Tang, X. Lin, Y. Xu, G. Chen, H. F. Kwok, Y. Lin and S. Feng, *J. Biophotonics*, 2019, **12**, e201800332.
- 156 W. Lee, A. Nanou, L. Rikkert, F. A. W. Coumans, C. Otto, L. W. M. M. Terstappen and H. L. Offerhaus, *Anal. Chem.*, 2018, **90**, 11290–11296.
- 157 W. Jia, P. Chen, W. Chen and Y. Li, *Medicine*, 2018, **97**, e12611.
- 158 J. Lin, L. Shao, S. Qiu, X. Huang, M. Liu, Z. Zheng, D. Lin, Y. Xu, Z. Li, Y. Lin, R. Chen and S. Feng, *Biomed. Opt. Express*, 2018, **9**, 984–993.
- 159 M. T. Gebrekidan, R. Erber, A. Hartmann, P. A. Fasching, J. Emons, M. W. Beckmann and A. Braeuer, *Technol. Cancer Res. Treat.*, 2018, **17**, 1–11.
- 160 M. Pinto, K. C. Zorn, J.-P. Tremblay, J. Desroches, F. Dallaire, K. Aubertin, E. T. Marple, C. Kent, F. Leblond, D. Trudel and F. Lesage, *J. Biomed. Opt.*, 2019, **24**, 025001.
- 161 K. Aubertin, J. Desroches, M. Jermyn, V. Q. Trinh, F. Saad, D. Trudel and F. Leblond, *Biomed. Opt. Express*, 2018, **9**, 4294–4305.
- 162 H. Chen, X. Li, N. Broderick, Y. Liu, Y. Zhou, J. Han and W. Xu, *J. Biophotonics*, 2018, **11**, e201800016.
- 163 H. Chen, X. Li, N. G. R. Broderick and W. Xu, *J. Raman Spectrosc.*, 2019, **51**, 323–334.
- 164 Q. Li, W. Li, J. Zhang and Z. Xu, *Analyst*, 2018, **143**, 2807–2811.
- 165 Z. Krbcova, J. Kukal, J. Mares, L. Habartova and V. Setnicka, *Biomed. Signal Process. Control*, 2019, **49**, 520–527.
- 166 P. Zuvela, K. Lin, C. Shu, W. Zheng, C. M. Lim and Z. Huang, *Anal. Chem.*, 2019, **91**, 8101–8108.
- 167 J. Desroches, M. Jermyn, M. Pinto, F. Picot, M.-A. Tremblay, S. Obaid, E. Marple, K. Urmey, D. Trudel, G. Soulez, M.-C. Guiot, B. C. Wilson, K. Petrecca and F. Leblond, *Sci. Rep.*, 2018, **8**, 1792.
- 168 K. Aubertin, V. Q. Trinh, M. Jermyn, P. Baksic, A.-A. Grosset, J. Desroches, K. St-Arnaud, M. Birlea, M. C. Vladoiu, M. Latour, R. Albadine, F. Saad, F. Leblond and D. Trudel, *BJU Int.*, 2018, **122**, 326–336.
- 169 M. Jermyn, K. Mok, J. Mercier, J. Desroches, J. Pichette, K. Saint-Arnaud, L. Bernstein, M.-C. Guiot, K. Petrecca and F. Leblond, *Sci. Transl. Med.*, 2015, **7**, 274ra219.
- 170 X. Feng, A. J. Moy, H. T. M. Nguyen, Y. Zhang, J. Zhang, M. C. Fox, K. R. Sebastian, J. S. Reichenberg, M. K. Markey and J. W. Tunnell, *J. Biomed. Opt.*, 2018, **23**, 057002.
- 171 D. V. Garcia, J. I. da Silva Filho, L. Silveira Jr, M. T. T. Pacheco, J. M. Abe, A. Carvalho Jr, M. F. Blos, C. A. G. Pasqualucci and M. C. Mario, *Vib. Spectrosc.*, 2019, **103**, 102929.

- 172 M. Yu, H. Yan, J. Xia, L. Zhu, T. Zhang, Z. Zhu, X. Lou, G. Sun and M. Dong, *Photodiagn. Photodyn. Ther.*, 2019, **26**, 430–435.
- 173 H. Yan, M. Yu, J. Xia, L. Zhu, T. Zhang and Z. Zhu, *Vib. Spectrosc.*, 2019, **103**, 102938.
- 174 E. Guevara, J. C. Torres-Galván, M. G. Ramírez-Elías, C. Luevano-Contreras and F. J. González, *Biomed. Opt. Express*, 2018, **9**, 4998–5010.
- 175 Y. A. Khrustoforova, I. A. Bratchenko, O. O. Myakinin, D. N. Artemyev, A. A. Moryatov, A. E. Orlov, S. V. Kozlov and V. P. Zakharov, *J. Biophotonics*, 2019, **12**, e201800400.
- 176 R. Sekine, S. Sato, J.-I. Tanaka, H. Kagoshima, T. Aoki and M. Murakami, *Showa Univ. J. Med. Sci.*, 2018, **30**, 381–389.
- 177 S. Sato, R. Sekine, H. Kagoshima, K. Kazama, A. Kato, M. Shiozawa and J.-I. Tanaka, *J. Anus Rectum Colon*, 2019, **3**, 84–90.
- 178 K. Aljakouch, Z. Hilal, I. Daho, M. Schuler, S. D. Krauß, H. K. Yosef, J. Dierks, A. Mosig, K. Gerwert and S. F. El-Mashtoly, *Anal. Chem.*, 2019, **91**, 13900–13906.
- 179 C. A. Jenkins, R. A. Jenkins, M. M. Pryse, K. A. Welsby, M. Jitsumura, C. A. Thornton, P. R. Dunstan and D. A. Harris, *Analyst*, 2018, **143**, 6014–6024.
- 180 M. Haifler, I. Pence, Y. Sun, A. Kutikov, R. G. Uzzo, A. Mahadevan-Jansen and C. A. Patil, *J. Biophotonics*, 2018, **11**, e201700188.
- 181 N. Stone, K. Faulds, D. Graham and P. Matousek, *Anal. Chem.*, 2010, **82**, 3969–3973.
- 182 N. Stone, M. Kerssens, G. R. Lloyd, K. Faulds, D. Graham and P. Matousek, *Chem. Sci.*, 2011, **2**, 776–780.
- 183 F. Nicolson, B. Andreiuk, C. Andreou, H.-T. Hsu, S. Rudder and M. F. Kircher, *Theranostics*, 2019, **9**, 5899–5913.
- 184 W. Wang, J. Zhao, M. Short and H. Zeng, *J. Biophotonics*, 2015, **8**, 527–545.
- 185 C. Kallaway, L. M. Almond, H. Barr, J. Wood, J. Hutchings, C. Kendall and N. Stone, *Photodiagn. Photodyn. Ther.*, 2013, **10**, 207–219.
- 186 B. C. Wilson, M. Jermyn and F. Leblond, *J. Biomed. Opt.*, 2018, **23**, 030901.